

Graduation thesis

# Characterisation of the LEDs and InGaAs detector of the handheld plastic scanner



Company supervisor: J. De Vos  
Physics supervisor: H. Van Hoorn  
Internship coach: R. Buning

Queena L.D. Rijke (18098258)  
Applied Physics  
June 1, 2023

**Abstract**

Plastic pollution is one of the most pressing problems worldwide, mainly due to the poor sorting process of the different types of plastic. Jerry de Vos made it his mission to develop a spectroscopy based technology that can separate the five most common types of plastic (PET, HDPE, PVC, LDPE, PP, PS), for those in developing countries. Jerry developed a handheld plastic scanner which uses a select number of LEDs in the NIR spectrum, each with a different wavelength, as the illumination light source and an InGaAs detector as the detector. The wavelength selection is done at the light source as opposed to between the light source and the detector in a spectrometer. To determine if the correct LEDs and InGaAs detector were chosen, the spectra of the LEDs were measured and plotted in the same graph as the responsivity of the InGaAs detector. The results showed that the 1460 nm and 1650 nm LED can be replaced. The 1460 nm LED can be replaced by a 1400 nm LED to increase the intensity around the identification dip around 1400 nm and the 1650 nm LED can be replaced by a 1650 nm LED with a higher power output. The 1720 nm LED can be removed from the plastic scanner design as the spectra of the LED overlaps with the spectra of the 1650 nm LED. Besides the characterisation of the spectroscopy components, the influence of the colour of a plastic has also been researched. The results showed that the darker coloured plastic samples have a less defined spectra, making it difficult to distinguish the types of plastic; therefore, it is recommended to remove these samples from the reference box provided by Plastic Scanner.

## Contents

<b>1</b>	<b>Introduction</b>	<b>1</b>
<b>2</b>	<b>Theory</b>	<b>3</b>
2.1	Molecular structure of plastics . . . . .	3
2.2	Infrared spectroscopy . . . . .	6
2.3	Light-emitting diodes . . . . .	8
2.4	InGaAs detector . . . . .	12
<b>3</b>	<b>Method</b>	<b>16</b>
3.1	LED characterisation . . . . .	17
3.2	InGaAs detector characterisation . . . . .	20
3.3	NIR reflection spectroscopy . . . . .	20
3.3.1	Halogen lamp and NIR spectrometer . . . . .	21
3.3.2	LEDs and NIR spectrometer . . . . .	23
3.3.3	Plastic scanner . . . . .	25
<b>4</b>	<b>Results</b>	<b>28</b>
4.1	LEDs and InGaAs detector characterisation . . . . .	28
4.2	Plastic identification . . . . .	31
4.2.1	Plastic characteristics . . . . .	33
4.3	Discussion . . . . .	33
<b>5</b>	<b>Conclusion</b>	<b>35</b>
5.1	Recommendations . . . . .	35
	<b>References</b>	<b>37</b>
	<b>Appendices</b>	<b>40</b>
<b>A</b>	<b>Enlarged figures</b>	<b>40</b>
<b>B</b>	<b>Spectra detection</b>	<b>44</b>
<b>C</b>	<b>Figures of the plastic characteristics</b>	<b>45</b>
<b>D</b>	<b>Intensity LEDs spectra</b>	<b>49</b>

## List of Figures

1.1	Plastic resin codes. . . . .	1
2.1	Molecular structures of five most common types of plastic. . . . .	3
2.2	Possible normal modes of a molecule. . . . .	4
2.3	The wavenumbers belonging to the absorption of molecule bonds. . .	5
2.4	The reflectance spectra of the five most common plastics. . . . .	6
2.5	The setup of the spectrometer to detect reflection or transmission. .	7
2.6	A schematic drawing of a LED pn-junction. . . . .	9
2.7	A simplified double heterostructure diode. . . . .	10
2.8	Different LED structures. . . . .	11
2.9	Spectral output of a LED. . . . .	12
2.10	A reverse biased photodiode pn-junction. . . . .	13
2.11	The theoretical responsivity of the InGaAs detector. . . . .	14
3.1	The internal design of the plastic scanner. . . . .	16
3.2	The side view of the internal design of the plastic scanner. . . . .	17
3.3	Schematic top view of the LED characterisation setup . . . . .	19
3.4	A screenshot of the WebPlotDigitizer program. . . . .	20
3.5	Schematic side view of the setup to identify the types of plastic using a halogen lamp as a light source. . . . .	22
3.6	Schematic side view setup to identify the types of plastic using LEDs as a light source. . . . .	24
3.7	The backside of the internal design of the spectroscopic side of the plastic scanner. . . . .	25
3.8	Schematic side and top view of the setup to identify the types of plastic using the plastic scanner. . . . .	26
3.9	A screen shot of the PS plot software. . . . .	27
4.1	The measured LED spectra and extracted responsivity of the InGaAs detector. . . . .	29
4.2	The FWHM values of the 8 different NIR LEDs . . . . .	30
4.3	The spectra of the five common types of plastic. . . . .	32
A.1	A screenshot of the PS plot software. . . . .	41
A.2	The spectra of the five common types of plastic measured with a halogen lamp as a light source. . . . .	42
A.3	The spectra of the five common types of plastic measured with LEDs as a light source. . . . .	42
A.4	The spectra of the five common types of plastic measured with the plastic scanner. . . . .	43
B.1	The spectra detection by the InGaAs detector. . . . .	44
C.1	The spectra of the five samples of PET. . . . .	45
C.2	The spectra of the five samples of HDPE. . . . .	46
C.3	The spectra of the six samples of PVC. . . . .	46
C.4	The spectra of the four samples of LDPE. . . . .	47
C.5	The spectra of the five samples of PP. . . . .	47
C.6	The spectra of the four samples of PS. . . . .	48

D.1 The intensity of the spectra from the LEDs . . . . .	49
--	----

## List of Tables

4.1 The peak wavelength values of the 8 different IR LEDs. . . . .	31
4.2 The plastic samples that are not suited as a reference. . . . .	33
C.1 The colours belonging to the letters in the legend. . . . .	45
D.1 The obtained power output of the LEDs from the data sheets. . . . .	49

## Abbreviations

**CB** Conduction band. 9, 11

**EHP** Electron-hole pair. 12–14

**FWHM** Full Width Half Maximum. 17, 28–30

**HDPE** High-Density PolyEthylene. i, 1, 3, 6, 21–23, 25, 27, 33, 44, 46

**InGaAs** Indium Gallium Arsenide. i, 2, 3, 13, 14, 16, 17, 20, 21, 27–29, 31, 35, 44

**IR** Infrared. 1, 4, 5, 7, 12, 34

**LDPE** Low-Density PolyEthylene. i, 21–23, 25, 27, 33–35, 47

**LED** Light Emitting Diode. i, 2, 3, 8–12, 16–19, 21, 23–25, 28–36, 44, 49

**NIR** Near-Infrared. i, 2, 4, 5, 16–25, 28, 31–34, 44, 49

**PET** PolyEthylene Terephthalate. i, 1, 3, 21–23, 25, 27, 45

**PP** PolyPropylene. i, 1, 3, 21–23, 25, 27, 35, 47

**PS** PolyStyrene. i, 1, 3, 21–23, 25, 27, 48

**PTFE** Polytetrafluorethylene. 7, 8, 21, 23, 26

**PVC** Poly Vinyl Chloride. i, 1, 3, 6, 21–23, 25, 27, 33, 46

**QE** Quantum Efficiency. 14

**SCL** Space Charge Layer. 13

**SNV** Standard Normal Variation. 21, 32

**VB** Valance band. 9, 11

## 1 Introduction

Plastic pollution is one of the most pressing problems worldwide. The gathering of plastics in nature negatively affects all living surroundings, humans and animals alike. Millions of animals are killed by plastics through starvation or entanglement and humans are currently being affected by the micoplastics in our food and water.

The popularity of plastics accelerated after World War II, because of its versatility, durability and affordability. Plastic has made space travel possible, revolutionised medicine and improved our safety with helmets and car lights. However, plastics are also used for everyday consumption, such as straws, grocery bags, bottles and more. Since the production and consumption of plastics increase faster than the degradation, the plastics are accumulating and end up on land or in various waters. The manufacturing of plastic increased exponentially from 2.3 million tons in 1950 to 448 million tons in 2015, and is expected to double by 2050 [1]. Plastic pollution is mostly visible in the developing countries, where recycling systems are inefficient or nonexistent [1–3].

The collecting and sorting process prior to recycling have proved especially problematic, mainly in the developing countries. Being able to separate the different types of plastic in a high-quality manner is important to ensure a successful recycling process. Each type of plastic is recycled with a different method, as each type consists of a different molecular structure. When sorting plastic, the plastic recycling codes can be checked located on the plastic material as triangles made of arrows. Within these arrows a number is given which states the type of plastic, see figure 1.1.



Figure 1.1: The plastic resin codes [4].

The five most common types of plastic are PET (PolyEthylene Terephthalate), HDPE (High-Density PolyEthylene), PVC (Poly Vinyl Chloride), PP (PolyPropylene) and PS (PolyStyrene). To distinguish the different types of plastic with a high quality, infrared (IR) spectroscopy can be used. However, sorting the plastic by means of IR spectroscopy is an expensive way to sort the different types of plastic, but this method can identify over 75% of the commonly used types of plastic. The different types of plastic can be identified by IR absorbance or IR reflectance [2, 5].

Jerry de Vos discovered during his thesis research that the sorting process of plastics is the most time consuming and labour-intensive [6]. Therefore Jerry made it his mission to develop a spectroscopy based technology that can separate the five most common types of plastic, for those in developing countries. The technology that is applied to develop the handheld plastic scanner is based on the technology developed by Armin Straller [7]. To increase the development process, the project has been set up as an open source project. All documentation, designs and progress is available at [plasticscanner.com](http://plasticscanner.com) [2, 8].

In spectroscopy, a broadband light source is used to illuminate the sample, after which the absorption or reflection spectrum is detected on a detector. Where the detector receives the intensity by wavelength. The handheld plastic scanner uses a select number of LEDs in the NIR spectrum, each with a different wavelength, as the illumination light source and an InGaAs detector as the detector. The wavelength selection is thus done at the light source as opposed to between the light source and the detector. Since the wavelength selection is made prior to the illumination, it is necessary to investigate whether the correct wavelengths have been selected to identify the different types of plastic. Next to using a less expensive light source for the plastic scanner development, a less expensive detector is used in the development. This involves researching whether the InGaAs detector can detect the wavelengths emitted by the LEDs. Besides the characterisation of the spectroscopy components, the influence of colour in plastic will be researched by means of the reflection spectra [9, 10].

For clarification, this report will answer the following research questions:

- How well do the spectra of the LEDs fit into the responsivity of the InGaAs detector?
- Which LEDs are suitable for the plastic scanner to be able to identify the different types of plastics?
- What detection range is needed for the InGaAs detector to be able to detect the identification dips of the spectra of the different types of plastic?
- Which plastic samples from the reference box provided by Plastic Scanner are suitable as a reference?

In order to determine whether the correct LEDs and detector are used and whether added colour affects the reflectance spectra of plastic, this report first describes the properties of plastic, LEDs and InGaAs detector and the operation of spectroscopy in the Theory. The method for the experiments is discussed in the Method after which the results are discussed. A conclusion is drawn from the results. Additional information can be found in the Appendices.

## 2 Theory

This chapter discusses the theory of the molecular structure of plastic, spectroscopy and the characteristics of LEDs and the InGaAs detector.

### 2.1 Molecular structure of plastics

Plastics are made out of polymers and can either occur as a natural or as a synthetic product. A polymer consists of multiple monomers bonded together. The plastics can be shaped when soft and can hold the shape when hardened [11–13]. Five of the most common plastics are: PET (PolyEthylene Terephthalate), PVC (Poly Vinyl Chloride), PP (PolyPropylene), PS (PolyStyrene) and HDPE (High-Density PolyEthylene), which are presented in figure 2.1.

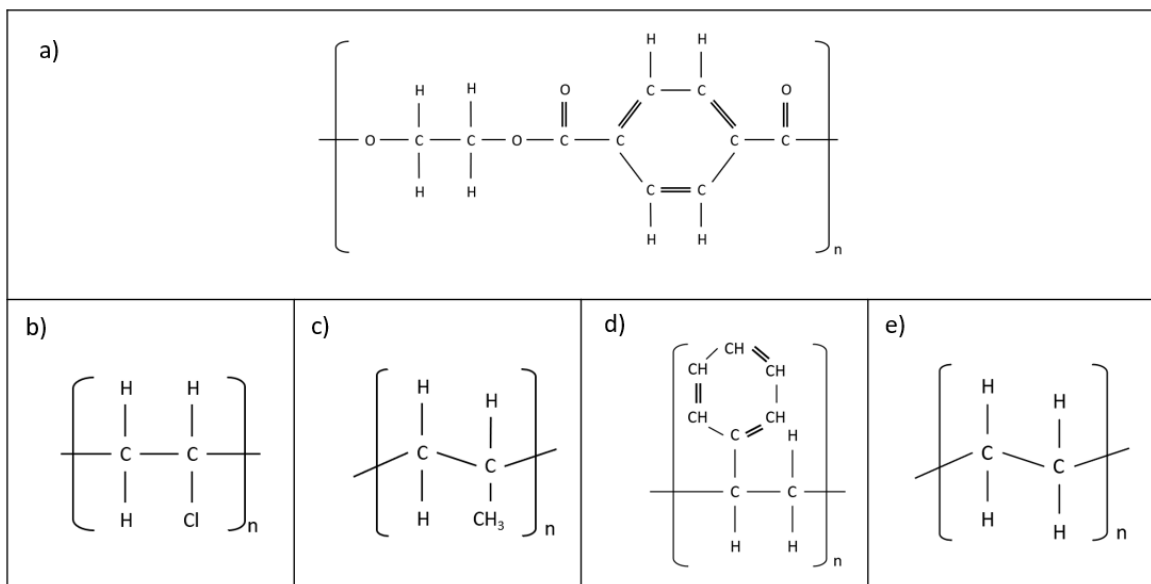


Figure 2.1: The molecular structures of the five most common types of plastic. a) shows the structure of PET, b) shows the structure of PVC, c) shows the structure of PP, d) shows the structure of PS and e) shows the structure of HDPE. [14–18]

The molecular structures can experience internal vibrations. Depending on the bonding between the atoms of the molecule, the molecule can vibrate in different directions. There are two types of vibrations: bending and stretching. The bending vibrations occur in four different directions, presented in cell A in figure 2.2. The stretching vibrations occur in two different directions, also presented in figure 2.2, in cell B.

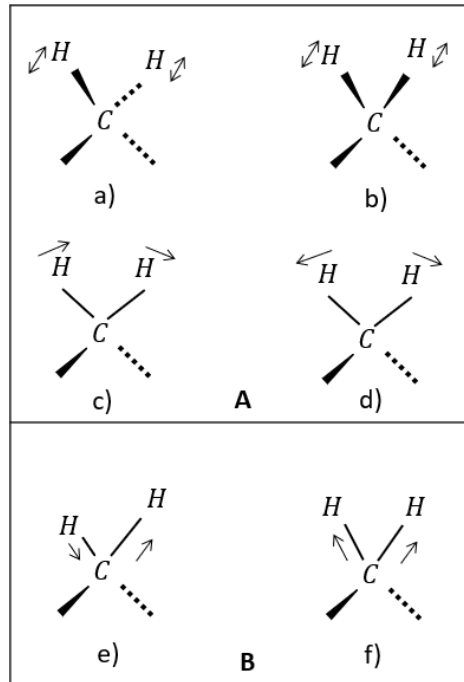


Figure 2.2: The bending vibrations are a) twisting, b) wagging, c) rocking and d) scissoring, presented in cell A. e) and f) are the asymmetrical and symmetrical stretching, presented in cell B.

These vibrations are known as normal modes, independent molecule vibrations. The frequencies of the normal modes are determined by the mass of the molecule atoms and its force constants. Multiple normal modes with the same frequency can occur in a molecule because of the symmetry inside the molecule. A molecule can absorb IR radiation when the normal mode vibrations cause a change in dipole moment. The vibration is then infrared-active [19].

Each absorption creates absorption bands forming an absorption spectrum. The C-H, O-H, N-H and C-O bonds characterise specific types of plastic by the absorbance in the NIR spectrum. The absorption bands in figure 2.3 are of the fundamental normal modes. When the monomers are bound into polymers, the vibrations become weaker and the absorption bands shift to the near infrared (NIR).

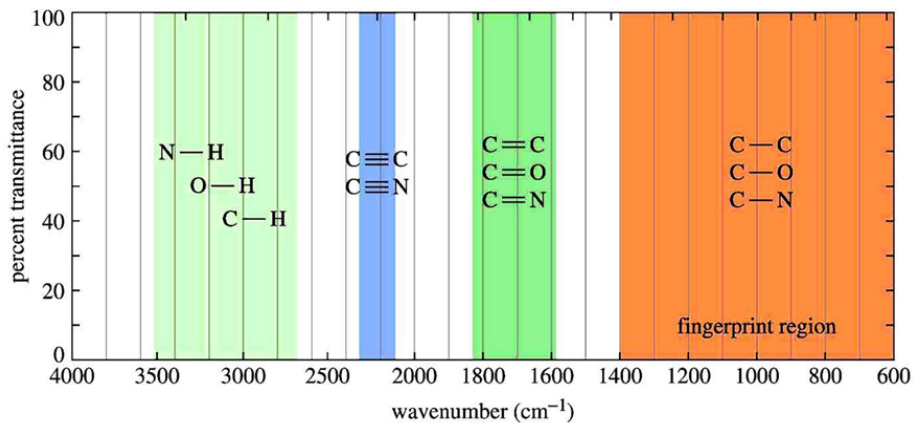


Figure 2.3: The absorption bands of specific C-bonds at a wavenumber range in the IR spectrum [20].

The IR spectrum ranges from 750 nm to 50 μm, in which the Near-infrared (NIR) ranges from 750 nm to 2.5 μm. These wavelengths are quite high and are therefore often written in wavenumbers. The wavenumber is a characterisation of the radiation in waves per centimetre, denoted by  $\sigma$ . The wavenumber,

$$\sigma = \frac{1}{\lambda} \quad (2.1)$$

in which  $\lambda$  is the wavelength in cm. The convenience of a scale in wavenumber is the linearity in energy [19].

Each type of plastic has multiple C-bonds which form an absorption spectrum. Figure 2.4 shows the absorption spectra of the different types of plastic. The spectra are shown with an offset to give a clear distinction between the types of plastic.

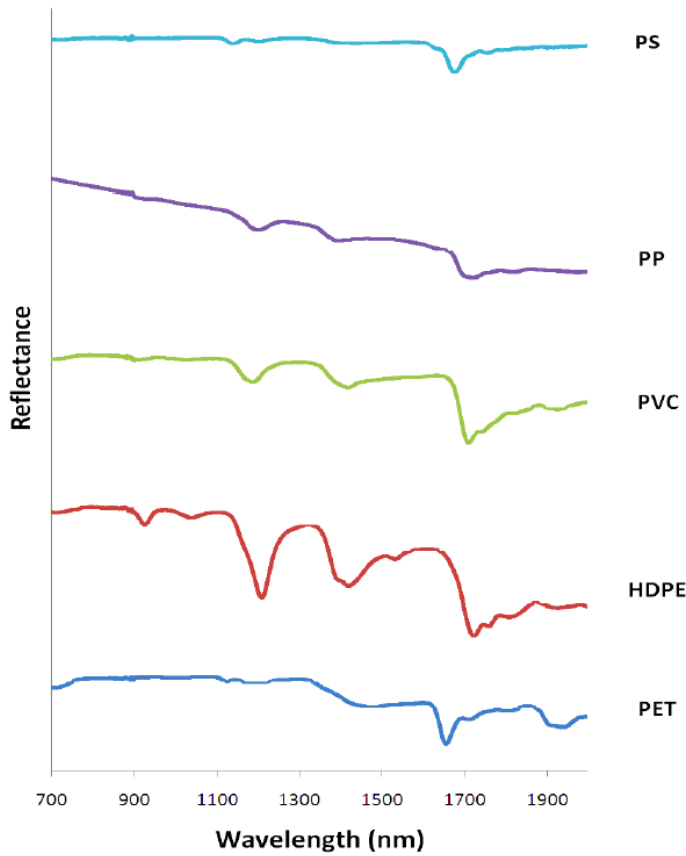


Figure 2.4: The reflectance of five of the most common types of plastic. The spectra are plotted with an offset to avoid interference and enhance clarity. The signature dips of the types of plastic are most present between 1100 nm to 1500 nm and around 1700 nm wavelength. [21]

Figure 2.4 shows that all the plastic types experience absorption between 1100 nm to 1500 nm and around 1700 nm. HDPE can be distinguished from PVC because of the absorption dip seen around 950 nm. The different spectra produced by the molecules of the plastics can be used for identification through reflectance spectroscopy [21].

## 2.2 Infrared spectroscopy

Spectroscopy is the study of the interaction between electromagnetic radiation and matter. The matter can absorb, reflect and transmit electromagnetic radiation depending on the frequency of the normal modes. The measuring of the electromagnetic radiation absorbed or emitted when atoms, molecules or ions of the matter undergo a state change, is called spectrometry. For measuring the electromagnetic radiation a spectrometer can be used, which consists of three basic elements: a light source, an element to isolate a narrow range of wavelengths and a detector. A spectrometer detects the transmission or reflection of a sample. The absorbance of a substance is measured by transmission and can be determined using the Beer-Lambert law [19],

$$A = \log_{10} \frac{I_0}{I_t} = -\log_{10} T = \varepsilon bc \quad (2.2)$$

in which  $I_0$  is the incoming intensity in  $\text{W m}^{-2}$ ,  $I_t$  is the transmitted intensity in  $\text{W m}^{-2}$ ,  $T$  is the transmission,  $\varepsilon$  is the molar absorption coefficient in  $\text{l mol}^{-1} \text{cm}^{-1}$ ,  $b$  is the path length in cm and  $c$  is the concentration in  $\text{mol l}^{-1}$  [19, 22, 23].

The concentration or path length of a substance affects the amount of transmission. A transmission obtained from a measurement between 30% and 70% is most accurate. A transmission higher than 75% indicates that the concentration is too low or the path length is too small [19].

Infrared (IR) spectrometry uses transmission or reflection to give an absorbance spectrum, by illuminating the sample with a light source in the IR spectrum. Certain wavelengths of the IR spectrum are absorbed by the normal modes of the sample and other wavelengths are reflected or pass through the sample. The difference in the setup determines if the reflection or transmission is measured by the detector in the spectrometer. An advantage of the reflection setup is that the thickness of the sample has no effect on the reflected spectrum, unless the thickness of the sample is smaller than the penetration thickness. An illustration is given in figure 2.5.

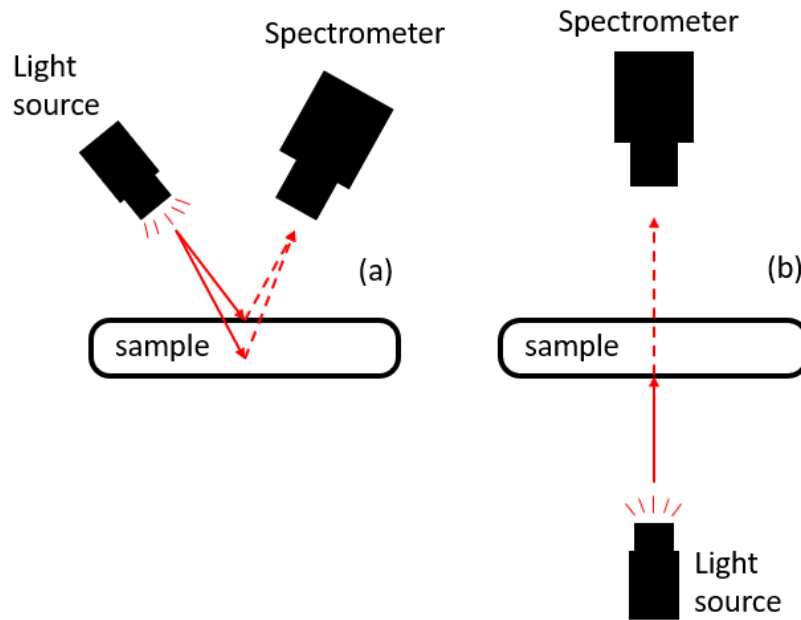


Figure 2.5: The setup of the spectrometer to detect reflection (a) or transmission (b).

The reflectance of a sample is determined by dividing the reference reflection of a reference tile, mainly made of PTFE, with the reflectance of the sample:

$$R = \frac{I_r}{I_0} \quad (2.3)$$

in which  $R$  is the reflectance,  $I_r$  is the intensity measured from the sample in counts and  $I_0$  is the reference intensity of the reference tile in counts. PTFE is used because of the material's high diffusivity. As a result, most of the illumination light is expected to be reflected.

When measuring the spectra of the different types of plastic, it is expected that the characteristics of the spectra will correspond with the characteristics shown in figure 2.4. It is also expected that the characteristics of the spectra will stay the same when measuring different colours of the same type of plastic, apart from dark colours where the characterising dips will diminish [9, 19, 21].

### 2.3 Light-emitting diodes

Light-emitting diodes (LEDs) are pn-junction diodes in which photon emission is generated as a result of a electron-hole pair recombination. A pn-junction diode is formed when a n-type semiconductor is joined to a p-type semiconductor. An n-type semiconductor is a doped crystal in which the negatively charged electrons carry the electric current, as a result of an excess in electrons. A p-type semiconductor is a doped crystal in which the electric current seems to be carried by the positively charged holes that the electrons leave when moving to a previous hole, as a result of a shortage in electrons [24].

Both semiconductors do not have a net charge. As a pn-junction a few of the electrons of the n-type fill the holes of the p-type, which causes the n-type to become positively charged and the p-type to be negatively charged. This region of depleted free carriers is called the depletion region and causes a potential difference inside the pn-junction, a built-in voltage ( $V_0$ ). The depletion region decreases when a forward bias is applied. Figure 2.6 demonstrates the flow of electrons and holes in equilibrium (a) and applied to a forward bias (b).

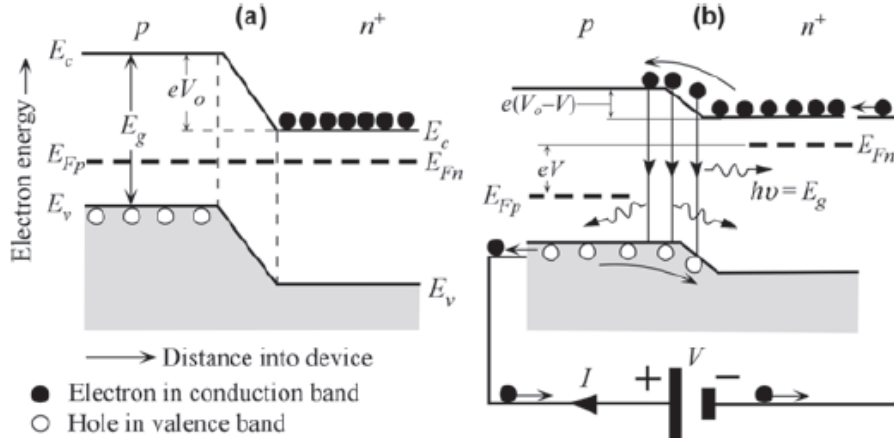


Figure 2.6: A schematic drawing of a pn-junction. The black circles represent the electrons in the conduction band (CB). The region in which the black circles (electrons) are located in figure 2.6. When the depletion region (dotted lines) between the conduction band and the valence band (VB) becomes smaller, the electrons can fill a hole in the valence band. The region in which the white circles (holes) are located in figure 2.6. The 'falling' of the electron from the bottom of the CB to the top of the VB is called recombination. During the process of recombination energy is released as a photon. A spontaneous emission of a photon. When connected to a forward bias a flow of spontaneous photon emissions takes place. The depletion region is then called the active region. The photons emitted in the active region have to escape the LED structure without being reabsorbed by the semiconductor material. Therefore the p-type side of the pn-junction needs to be very narrow, or a heterostructure can be used. [24]

The free electrons are located in the conduction band (CB). The region in which the black circles (electrons) are located in figure 2.6. When the depletion region (dotted lines) between the conduction band and the valence band (VB) becomes smaller, the electrons can fill a hole in the valence band. The region in which the white circles (holes) are located in figure 2.6. The 'falling' of the electron from the bottom of the CB to the top of the VB is called recombination. During the process of recombination energy is released as a photon. A spontaneous emission of a photon. When connected to a forward bias a flow of spontaneous photon emissions takes place. The depletion region is then called the active region. The photons emitted in the active region have to escape the LED structure without being reabsorbed by the semiconductor material. Therefore the p-type side of the pn-junction needs to be very narrow, or a heterostructure can be used.

To create a heterostructure multiple heterojunctions are combined. A heterojunction are two different semiconductor crystals, with different bandgap energy, joined together. In this case a pn-junction. By combining pn-junctions a dielectric waveguide can be formed to guide the emitted photons out of the active region. The difference between the bandgaps can be increased by altering the refractive index of the semiconductor material and in doing so the LED intensity increases. Figure 2.7 shows an example of a double heterostructure.

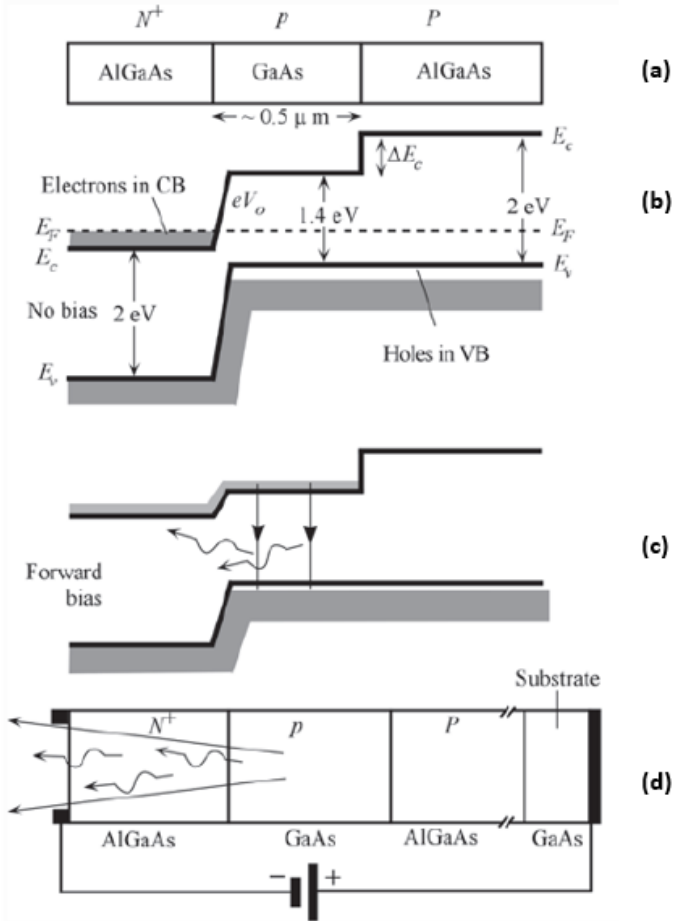


Figure 2.7: A simplified double heterostructure diode. (b) shows an energy band diagram in which the features are exaggerated, (c) shows a forward-biased energy band diagram, (d) a forward-biased LED, in which the escaping of the emitted photons is illustrated. [24]

Not all light rays can leave the heterostructure waveguide, because of total internal reflection on the semiconductor-air interface. By reshaping the surface of the semiconductor more light can leave the structure. A dome or hemisphere could be used to change the angle in which the light strikes the semiconductor-air interface and therefore more light can be emitted. More common used techniques to increase emission of light is to encapsulate the semiconductor within a transparent plastic medium or to texture the surface. A distributed Bragg reflector could also be used to increase the extraction ratio of the LED's wavelength or a resonant cavity could be used as a LED design. These LED designs are shown in an exaggerated form in figure 2.8.

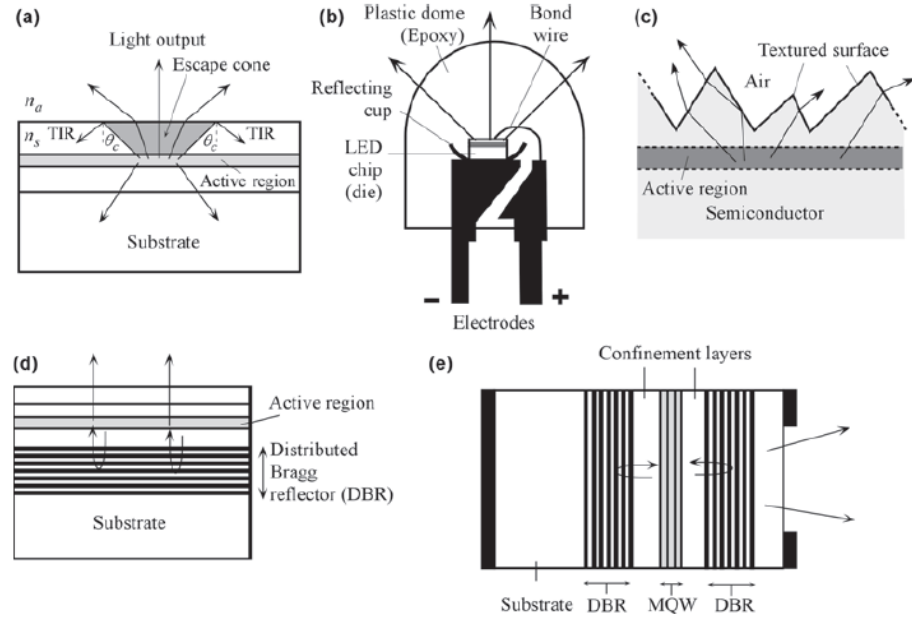


Figure 2.8: Five different designs to increase the intensity of a LED. The plastic dome (b) is used to increase the intensity of the LEDs used in the plastic scanner. [24]

The plastic dome design (2.8b) is used for the design of the LEDs used in the plastic scanner.

The output spectrum of the LED is next to the dependence of the semiconductor material and the structure of the pn-junction also dependent on the dopant concentrations. The semiconductors are typically not heavily doped to generate photons with a higher energy than  $E_g$  and to acquire a sharp edge between the energy of the CB and the energy of the VB. The emission of the output spectrum can be described as follows,

$$\begin{aligned} h\nu_0 &\approx E_g + \frac{1}{2}k_B T \\ h\Delta\nu &= m k_B T \end{aligned} \tag{2.4}$$

in which

$h$	constant of Planck	$6.626 \cdot 10^{-34} \text{ Js}$
$\nu_0$	peak emission frequency	Hz
$E_g$	bandgap energy	eV
$k_B$	Boltzmann constant	$1.3807 \cdot 10^{-23} \text{ J K}^{-1}$
$T$	temperature	K
$\Delta\nu$	spectral width	Hz
$m$	numerical factor	-

The value for  $m$  for many LEDs is  $m \approx 3$ . Typically the value varies between 1.5 and 3.5. Equation 2.4 can be written in terms of wavelength  $\lambda_0$  or spectral width  $\Delta\lambda$ . Both wavelength and spectral width increase with an increase in temperature. This can be seen in figure 2.9 [24, 25].

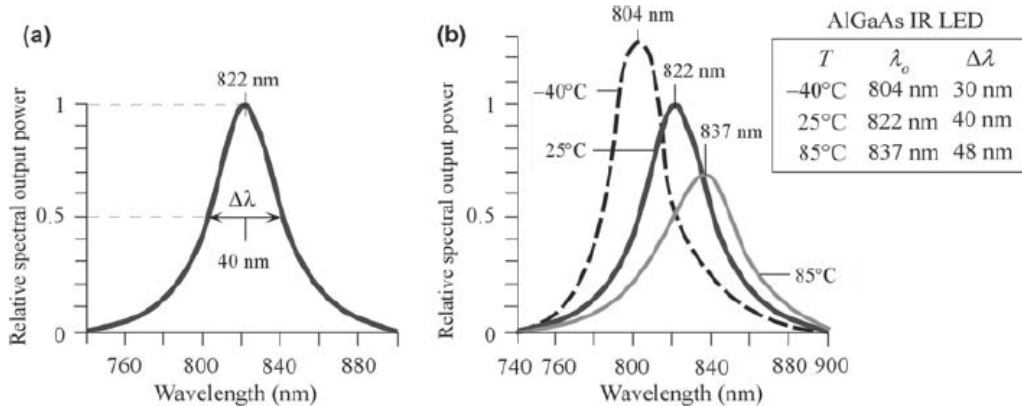


Figure 2.9: The output spectrum of an IR AlGaAs LED. (a) shows the typical output spectrum of the AlGaAs LED and (b) shows the shifting of the output spectrum with increase in temperature. [24]

## 2.4 InGaAs detector

A photodiode is a pn-junction in which photons are absorbed to generate electron-hole pairs (EHP). Compared to the LED pn-junction the photodiode has a  $p^+$ -type as to the  $n^+$ -type of the pn-junction of the LED. The plus-sign in the  $p^+$ -type, means that the concentration of acceptors is greater than the donor concentration in the n-type. The pn-junction of the photodiode too has a built-in voltage. By applying a reverse bias to the pn-junction the depletion region becomes greater, which gives more space for EHP photogeneration.

A free EHP is created when a photon is absorbed in the depletion region. The electron and hole drift toward the opposite side of the pn-junction and generate a current, the photocurrent  $I_{ph}$ . The duration of the current is as long as the electron and hole drift. The electron and hole drift are visually represented in figure 2.10 after the absorbance of a photon under a reverse bias.

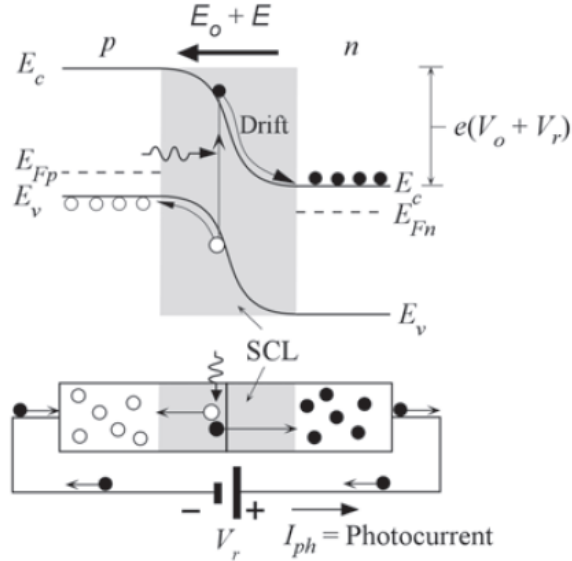


Figure 2.10: A reverse biased pn-junction in which a free EHP is generated by the absorbance of a photon. The photogeneration takes place in the depletion region (SCL). The free electron and hole drift causing a photocurrent  $I_{ph}$ . [26]

For the photon to be absorbed and generate an EHP, the energy of the photon needs to be at least equal to the energy of the bandgap  $E_g$  of the semiconductor material. The wavelength of the photon therefore depends on the bandgap energy. The threshold wavelength of the photon can be determined using the following equation:

$$\lambda_g(\mu\text{m}) = \frac{1.24}{E_g(\text{eV})} \quad (2.5)$$

in which  $\lambda_g$  is the threshold wavelength in  $\mu\text{m}$  and  $E_g$  the bandgap energy in eV. The plastic scanner uses an InGaAs photodiode. The values of the threshold wavelength and the bandgap energy corresponding to the InGaAs detector are  $E_g = 0.75 \text{ eV}$  and  $\lambda_g = 1.65 \mu\text{m}$ .

The light intensity of the photons with a wavelength shorter than  $\lambda_g$  decays exponentially over a distance into the semiconductor. The distance over which the most absorption takes place is called the penetration or absorption depth ( $\delta$ ). The absorption depth can be determined through the absorption coefficient.

$$\delta = \frac{1}{\alpha} \quad (2.6)$$

in which  $\alpha$  is the absorption coefficient in  $\text{m}^{-1}$ .

With a large absorption coefficient the photogeneration will take place near the surface of the  $p^+$ -layer and when the absorption coefficient is too small the number of generated EHPs decreases in the depletion region. A greater efficiency is reached

when the photogeneration takes place in the depletion region. The efficiency of the absorption in the depletion region can be determined with the following equation,

$$\eta_e = \frac{I_{ph}/e}{P_0/h\nu} \quad (2.7)$$

in which  $\eta_e$  is the device quantum efficiency (QE),  $I_{ph}$  is the photocurrent in A and  $P_0$  is the incident optical power in W.

Not all incident photons generate free EHPs that are collected to induce a photocurrent, when absorbed on the photodiode. Some disappear by recombination, get trapped or reflect on the air-semiconductor interface. The performance of the photodiode is characterised by its responsivity, photocurrent per incident optical power.

$$R = \frac{I_{ph}}{P_0} = \eta_e \frac{e\lambda}{hc} \quad (2.8)$$

in which  $R$  is the responsivity in A/W,  $\lambda$  is the wavelength in m and  $c$  is the speed of light  $2.998 \cdot 10^8$  m/s. As seen in equation 2.8, the responsivity is depended on the wavelength. It is therefore often represented in a  $R$  vs.  $\lambda$  graph, which is usually provided by the manufacturer. The theoretical responsivity of the InGaAs detector is presented in figure 2.11.

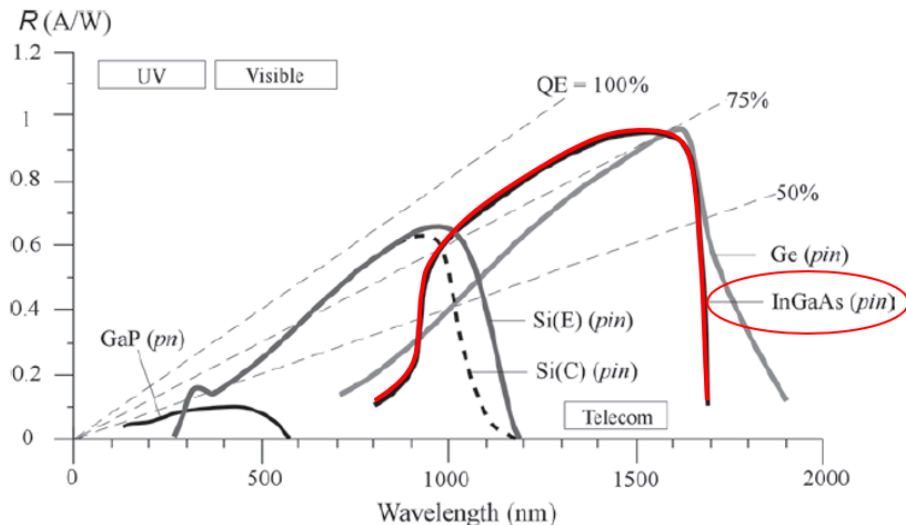


Figure 2.11: The red line is the responsivity of the InGaAs detector. The detection range is from 800 nm to 1700 nm. [26]

The shape of the curve in figure 2.11 is depended on the structure of the device, the absorption coefficient and the QE.

The responsivity of the InGaAs detector in figure 2.11 is of a pin photodiode. The biggest advantage of a pin photodiode is the wider depletion region allowing a larger

amount of photogeneration can take place. For this reason the responsivity is better than a pn-junction photodiode [26].

### 3 Method

The plastic scanner is a spectrometer which illuminates the sample with 8 different LEDs. Each LED has a different wavelength inside the NIR spectrum. The plastic sample is illuminated in turns by each LED. The internal design of the plastic scanner is presented in figure 3.1.

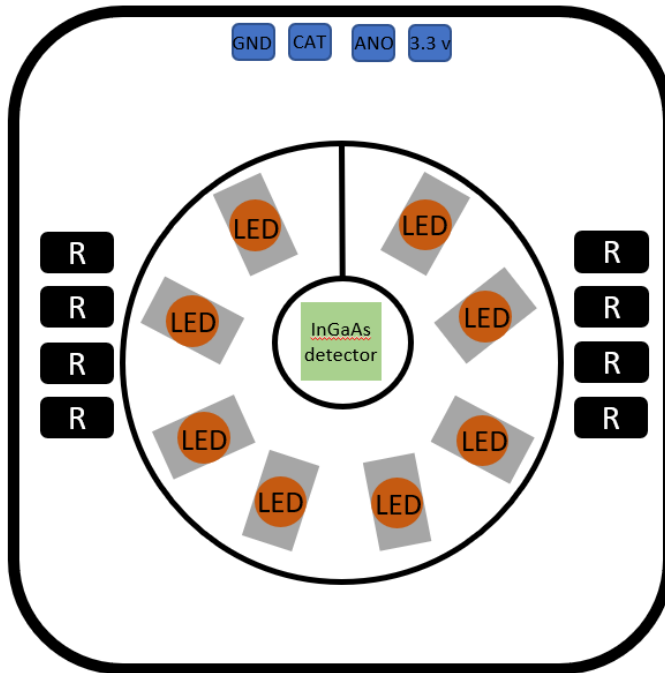


Figure 3.1: The internal design of the spectroscopic side of the plastic scanner. The InGaAs detector is surrounded by 8 LEDs, each emitting light in an different wavelength. The resistors for the LEDs are placed on the sides of the board (R). The Arduino, to manage the LEDs and analyse the reflected spectra collected from the InGaAs detector, is connected via the four connectors at the top of the board. The GND and 3.3v deliver the voltage to the board and the CAT and ANO are the connectors for the detector. The circle around the LEDs is the spacer between the plastic samples and the LEDs, usually 10 mm high. The circle around the InGaAs detector is used to block any direct light from the LEDs into the detector, usually 4 mm high.

A side view of the internal design to show the placement of the spacer is presented in figure 3.2.

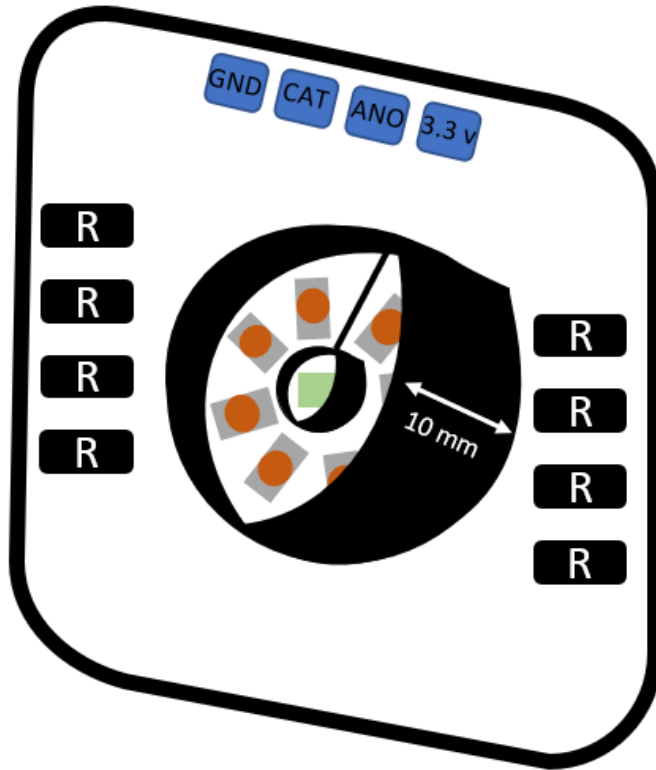


Figure 3.2: A side view of the internal design of the spectroscopic side of the plastic scanner. The LEDs are surrounded by a 10 mm high spacer. The InGaAs detector is surrounded by a 4 mm high spacer to block any direct light emitted from the LEDs.

A discrete spectrum of a plastic sample is measured at specific wavelengths. To determine if the plastic samples can be identified using the plastic scanner, a reference of the spectra of the plastic samples is made using a NIR spectrometer and a broadband light source for illumination. By characterising the components, the LEDs and the InGaAs detector, the efficiency and accuracy of the plastic scanner can be determined.

First the characterisation of the LEDs and InGaAs detector will be discussed. Second the measuring method to determine the spectra of the plastic samples will be discussed.

### 3.1 LED characterisation

Of most LEDs the spectra, FWHM and peak wavelengths are known from the data sheet. Because not all data is known from all LEDs, the spectra will be measured using a spectrometer as detector. The equipment needed to build the setup are as follows:

- Optical multimode fibre (FC-UVIR400-1-ME)
- NIR LED development board

- LED development board ( $\lambda = 576$  nm)
- Board with switches
- Power supply (Velleman LABPS1503)
- Cables to connect the LED development board to a board with switches
- Cables to connect the board with switches to the power supply
- Computer to run the Avasoft8 software
- Optical plate
- Avantes NIR spectrometer (AVASPEC-NIR256-2.0TEC)
- Avantes spectrometer (AVASPEC-ULS2048CL-EVO-RS)
- Lens (Thorlabs LSB04-A  $\varnothing 1"$  N-BK7,  $f = 25.4$  mm)
- USB-A to USB-B cable
- SMA mounts to hold the fibre ends
- Lens mount

## Setup

The setup to characterise the LEDs is built according to figure 3.3. The lens is placed between the LED development board and the first fibre mount. An optical multimode fibre can be attached to the second fibre mount or the NIR spectrometer. The dotted line suggests the different connections of the fibre. It can either be connected to the second fibre mount or the spectrometer.

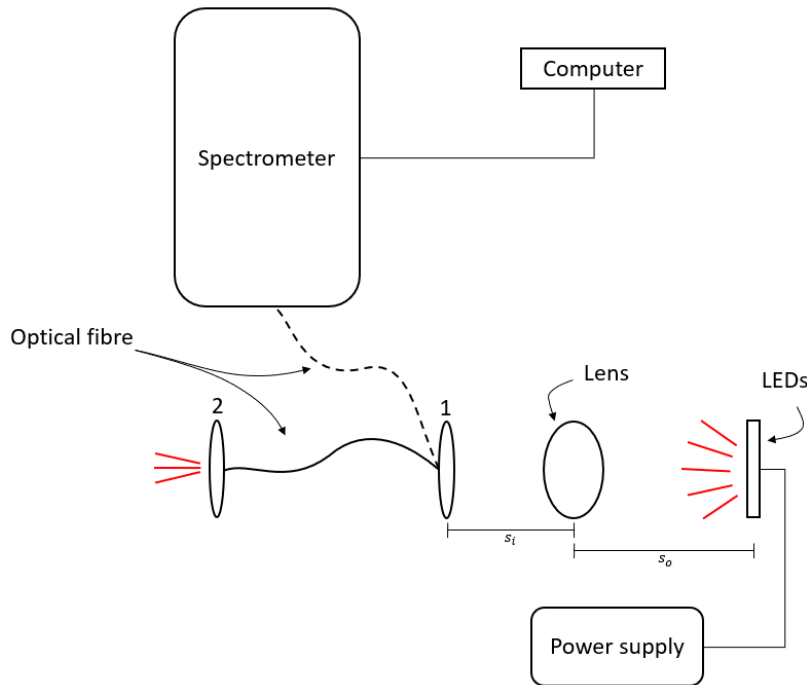


Figure 3.3: A schematic top view of the setup to determine the spectra of the LEDs. The lens is placed at an object distance  $s_o$  and the fibre is placed after the lens, connected to fibre mount 1, at an image distance of  $s_i$ . The fibre can be either connected to the NIR spectrometer or fibre mount 2, suggested by the dotted line. The NIR spectrometer is connected to a computer containing AvaSoft8 software.

To measure the spectra of the LEDs, the light of the LEDs is focused by a lens into the fibre which is connected to the spectrometer. By using a LED development board with LEDs in the visible spectrum, the LEDs can be aligned. The LED development board is connected to a board with switches. Each switch lights a different LED on the board. The power supply is set at a voltage of 3.3 V. When a LED is correctly aligned the light is transmitted to through the fibre and is visible on a screen or a finger held before fibre mount 2. After alignment the LEDs within the visible spectrum are replaced with the LEDs in the NIR spectrum. The fibre is then connected to the spectrometer and the spectrum of the aligned LED can be measured. The integration time and the average in the AvaSoft8 programme for the NIR spectrometer will be determined by aligning the 1550 nm LED into the NIR spectrometer (due to its high power output) and press the auto configuration button **Jac**. The wavelength range goes from 1000 nm to 2000 nm. The integration time and the average in the AvaSoft8 programme for the spectrometer will be determined by aligning the 940 nm LED into the spectrometer and press the auto configuration button **Jac**. The wavelength range goes from 300 nm to 1100 nm.

The data is manually saved in Excel-documents and plotted using Python.

### 3.2 InGaAs detector characterisation

The characterisation of the InGaAs detector cannot be improved compared to the responsivity given in the data sheet, because the necessary materials to accurately measure the responsivity are not available. Hence the data from the data sheet will be used for the characterisation of the plastic scanner.

#### Setup

The plotted data of the responsivity of the detector has been extracted using an online program named WebPlotDigitizer [27]. Figure 3.4 shows a picture of the program.

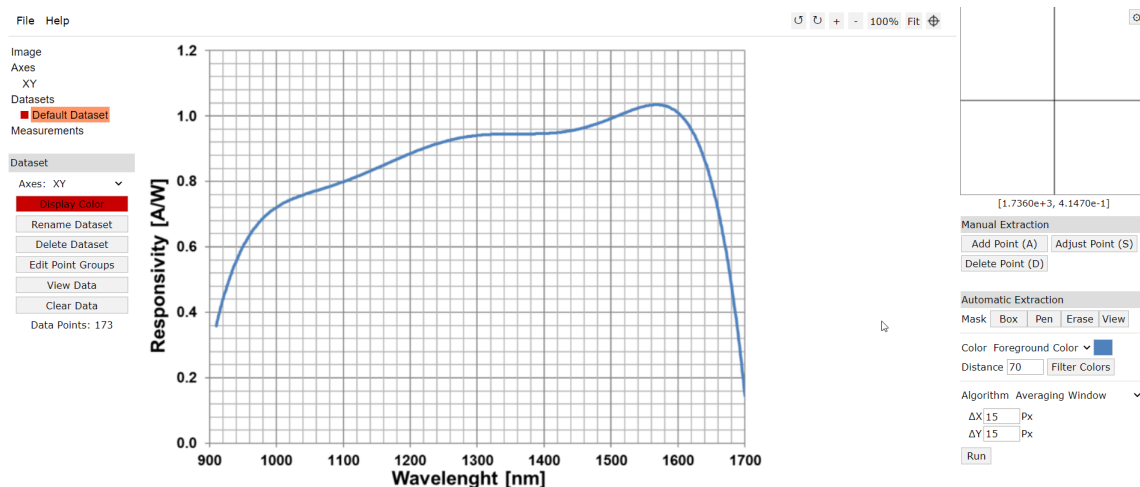


Figure 3.4: A screenshot of the WebPlotDigitizer program. It shows the uploaded graph in the middle. The way to extract the data from the uploaded graph are presented on the right side. On the left side, the extracted data can be viewed and downloaded.

Within the program an image of the graph given in the data sheet is uploaded. To determine the values of the curve of the graph, the minimum and maximum values of the x- and y-axis are determined by selecting and entering the minimum and maximum values into the designated areas on the website. Once the outline of the graph is established the curve of the responsivity is selected using the pen function. The colours are then filtered on a distance value of 70, using the colour picking function to determine the colour code of the curve. The  $\Delta X$  and  $\Delta Y$  are set on 15 Px. Then the program can be run and the data is given in dots on the graph and can be viewed by clicking on the "View Data" button. The acquired data can be adjusted in the formatting and saved as a CSV-document.

### 3.3 NIR reflection spectroscopy

The spectra of the plastic samples are measured in three different ways. As a reference the spectra are measured using a halogen lamp as the illumination source and a NIR

spectrometer as the detector. The spectra are also measured using the LEDs as the illumination light source with the NIR spectrometer as the detector. In final the spectra are measured with the plastic scanner using the LEDs as the illumination light source and the InGaAs detector as the detector. For all experiments the measured spectra of the plastic samples are SNV filtered. The data is filtered with the following equation:

$$\text{output data} = \frac{\text{input data} - \text{mean input data}}{\text{standard deviation}} \quad (3.1)$$

in which the output data is the SNV-filtered data, the input data is the measured data set of one plastic sample, the mean input data is the determined mean of the input data set and the standard deviation is the determined standard deviation of the input data set. By SNV filtering the data is compensated for the different reflection intensities [28].

### 3.3.1 Halogen lamp and NIR spectrometer

The NIR spectra of the types of plastic can be measured with a NIR spectrometer, a broadband light source and an optical reflection probe. The probe is able to illuminate the plastic and detect the reflected NIR spectra. The equipment needed to execute the experiment are as follows:

- Plastic sample reference box C (containing PET, HDPE, PVC, LDPE, PP and PS)
- Avantes NIR spectrometer (AVASPEC-NIR256-2.0TEC)
- Halogen lamp (AVALIGHT-HAL LS-1108038)
- Optical reflection probe (FCR-7IR200-2-ME)
- USB-A to USB-B cable
- Stand to hold the probe
- Reference tiles (Avantes, Plastic Scanner, paper sheet, PTFE, Spectrapod)
- Computer/Laptop containing AvaSoft8 software

### Setup

The setup is built according to figure 3.5. The probe is connected to the light source and the NIR spectrometer. The end of the probe is held by a clasp to be able to detect the NIR spectrum of the plastic sample from above.

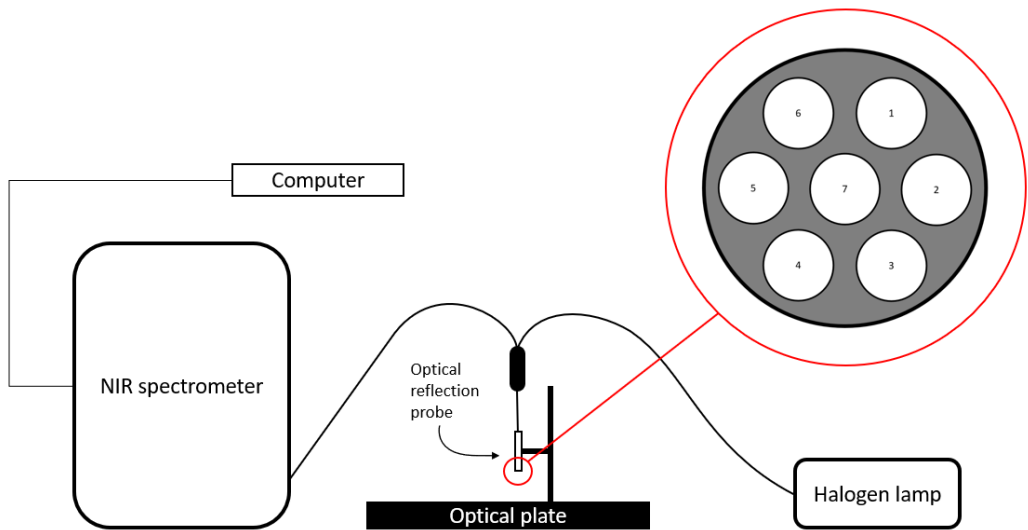


Figure 3.5: A schematic side view of the setup to identify the types of plastic using a NIR spectrometer. An optical reflection probe is connected to the halogen lamp light source and the NIR spectrometer. The ending of the probe is placed in such a way that it can illuminate and detect the plastic samples on the plate. The six fibres inside the probe illuminate the sample and the seventh fibre detects the reflected spectra. A clasp is used to hold the probe ending at a distance of 10 mm from the optical plate. The NIR spectrometer is connected to a computer/laptop containing the AvaSoft8 software.

Before measuring, the integration time and average of the Avantes spectrometer are set. The integration time is set on a value of 80.000 ms and the average is set on a value of 1. The Dynamic Dark in the same settings is disabled. The range of the wavelength in which the spectrometer will measure are set from 1000 nm to 1900 nm. A dark measurement is made and saved in AvaSoft8.

First the reference tiles are measured. The reference tile is placed under the probe ending with a distance in between of 10 mm. The tile is measured five times, where at each measurement a different location on the tile is measured. By measuring the tile five times at different locations, the random error of the experiment is taken into account. After measuring each reference tile, the plastic samples provided by Plastic Scanner are measured. Six different plastic types are present in reference box C: PET, HDPE, PVC, LDPE, PP and PS. Each bag consists of four to six samples of one type of plastic. Each sample of the plastic type is measured five times at different locations on the sample. The plastic samples are placed on top of the reference tile that will be used during the experiment. The samples are measured in a continuous scan of the spectrometer.

The data is manually saved in Excel-documents during each measurement and plotted using Python.

### 3.3.2 LEDs and NIR spectrometer

The NIR spectra of the types of plastics are detected using a spectrometer and are illuminated with NIR LEDs. An optical multimode fibre is connected between the spectrometer and the LED development board. The equipment needed to measure the spectra of the plastics are as follows:

- Avantes NIR spectrometer (AVASPEC-NIR256-2.0TEC)
- Optical multimode fibre (FC-UVIR400-1-ME)
- NIR LED development board with SMA connection
- Plastic sample reference box C (containing PET, HDPE, PVC, LDPE, PP and PS)
- Reference tiles (Avantes, Plastic Scanner, paper sheet, PTFE, Spectrapod)
- USB-A to USB-B cable
- Computer/laptop containing Avasoft8 software
- Board with switches
- Power supply (Velleman LABPS1503)
- Stand to hold the LED development board
- Cables to connect the LED development board to the board with switches
- Connection cables for the board with switches and the power supply

### Setup

The basis of the setup is derived from figure 3.5. In this setting a single fibre is connected between the LED development board and the spectrometer in which the spectrometer is used as the detector. A schematic view of the setup is presented in figure 3.6.

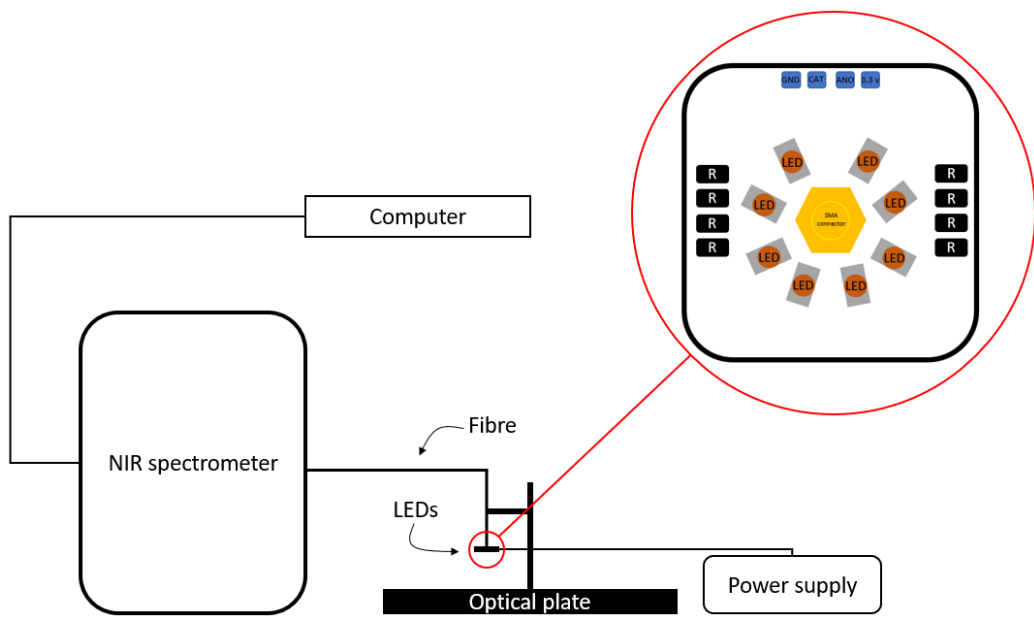


Figure 3.6: A schematic side view of the setup to measure the spectra of the types of plastics using NIR LEDs as the light source. The LEDs are connected to a power supply through a board with switches. The switches can be used to light each LED individually or simultaneously. The spectrometer is connected to a computer containing the Avasoft8 software.

The LED development board and the board with switches are mounted to the optical table. The two boards are connected via three electronic cables, placed on the position A, B and C shown in figure 3.7. The board with switches is connected to the power supply on which the voltage is set at 3.3 V. The LED development board is via the SMA connector, shown in figure 3.7, connected to the NIR spectrometer with an optical fibre. The spectrometer is connected to the computer to measure the reflected spectra from the plastic samples.

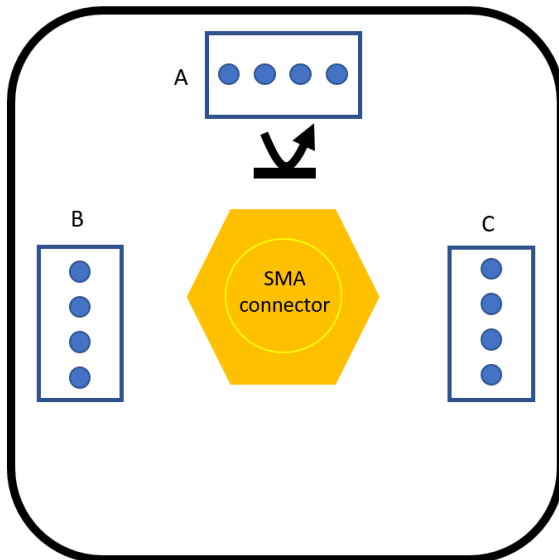


Figure 3.7: The backside of the internal design of the spectroscopic side of the plastic scanner. The blue rectangles (A, B and C) are used to connect the board with the Arduino via the three electronic cables. The optical fibre is connected between the board and the NIR spectrometer using the SMA connector attached to the board.

The LEDs are connected to the board with switches which is connected to the power supply. All LEDs are switched on while measuring the spectra of the reference tiles and plastic samples. First the spectra of the reference tiles are measured by placing each tile under the LED development board at a distance of 10 mm. Each tile is measured five times at different locations to account for the random error. After the spectra of the tiles are measured the spectra of the plastic samples from reference box C, containing: PET, HDPE, PVC, LDPE, PP and PS, are measured. The reference tile provided by Plastic Scanner is placed under each plastic sample during the measurements. The spectra of each plastic sample is also measured five times at different location on the sample. Both, the reference tiles and the plastic samples, are measured in a continuous scan of the NIR spectrometer.

The data is manually saved in Excel-documents during each measurement and plotted using Python.

### 3.3.3 Plastic scanner

The spectra of the types of plastic are measured using the prototype of the plastic scanner. The plastic scanner is controlled by the PS plot program available on GitHub. The equipment needed to measure the spectra of the plastic with the plastic scanner are as follows:

- Plastic scanner prototype #01
- Plastic sample reference box C (containing PET, HDPE, PVC, LDPE, PP and PS)

- Reference tiles (Avantes, Plastic Scanner, paper sheet, PTFE, Spectrapod)
- USB-A to USB-B cable
- Computer/laptop containing PS plot software

## Setup

Figure 3.8 shows a schematic view of the setup for executing the experiment.

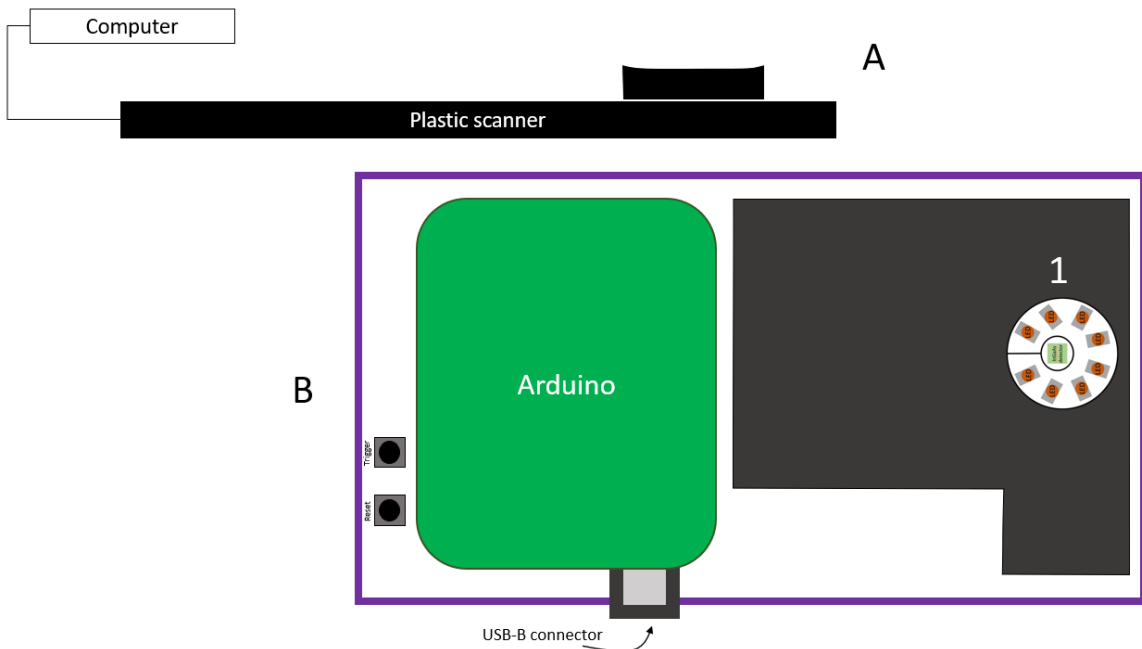


Figure 3.8: A schematic side and top view of the setup to identify the types of plastic using the plastic scanner. **A** is the side view of the plastic scanner. **B** is the top view of the plastic scanner in which **1** is the scanning area. The increment in **A** represents the 10 mm spacer of **1**. The plastic scanner is through the USB-B connector via a USB-A to USB-B connector connected to the computer.

The prototype of the plastic scanner is connected to a computer containing the PS plot software which can be found on GitHub [29]. To use the real data in PS plot, the correct COM-port needs to be selected. This can be done at the top of program format, see figure 3.9.

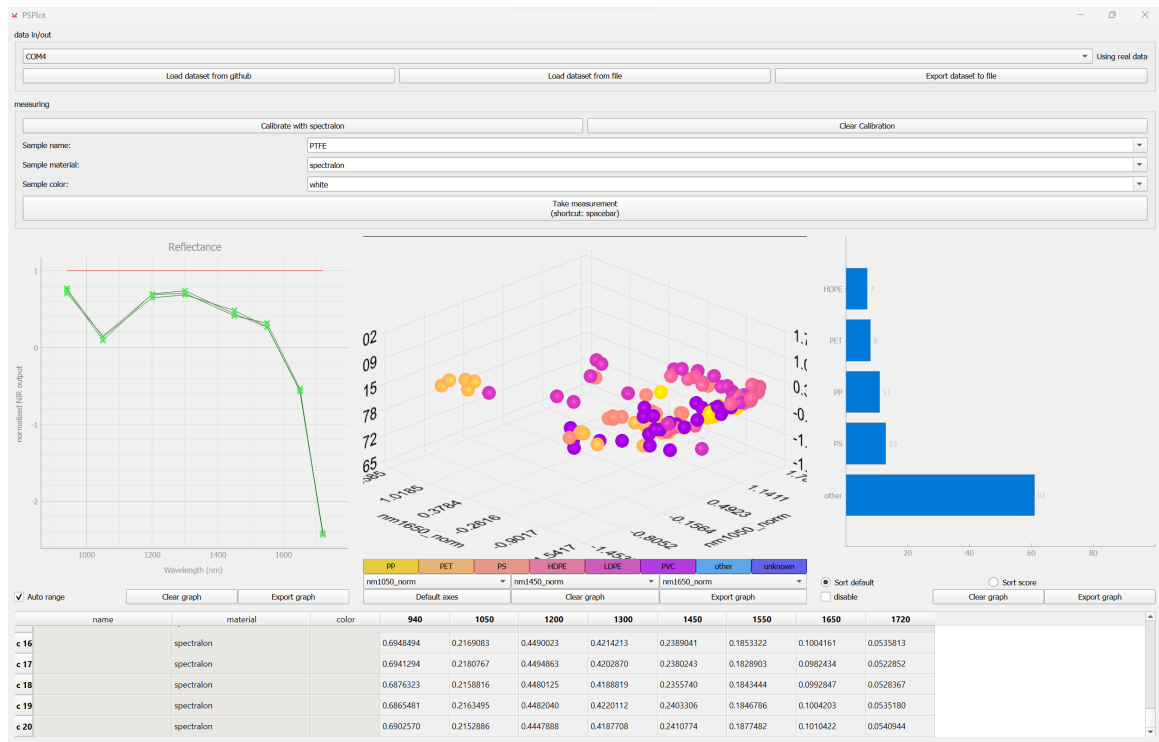


Figure 3.9: A screen shot of the PS plot program. The graph on the left shows the measured spectra of the samples with the red line as the reference. The middle graph shows the measurement points in a 3D plot with the axis indicating the intensity of the dips in the spectra. The right graph is a probability graph, in which the bars indicate by what percentage the sample corresponds to a type of plastic. The data underneath the graphs are the raw output of the InGaAs detector. An enlarged figure can be found in appendix A.

The reference tiles are measured before the plastic samples. Each tile is placed on top of the scanning area (**1** in figure 3.8). By pressing the "Calibrate with spectralon" button, a measurement of the reference tile will be taken. The red line in the left graph will appear. After calibrating, the plastic samples from reference box C, containing PET, HDPE, PVC, LDPE, PP and PS, can be measured by laying the samples on the scanning area and putting the reference tile on top of the sample. The identification code and features of the sample can be put in the bars above the measurement button. Each reference tile and plastic sample will be measured five times. After each five measurements the data is manually copied, pasted and saved in a .txt-file. At the end of all measurements the data can be exported to a .csv-file using the "Export dataset to file" button in the right corner. The data from the .txt-files is then processed in Python.

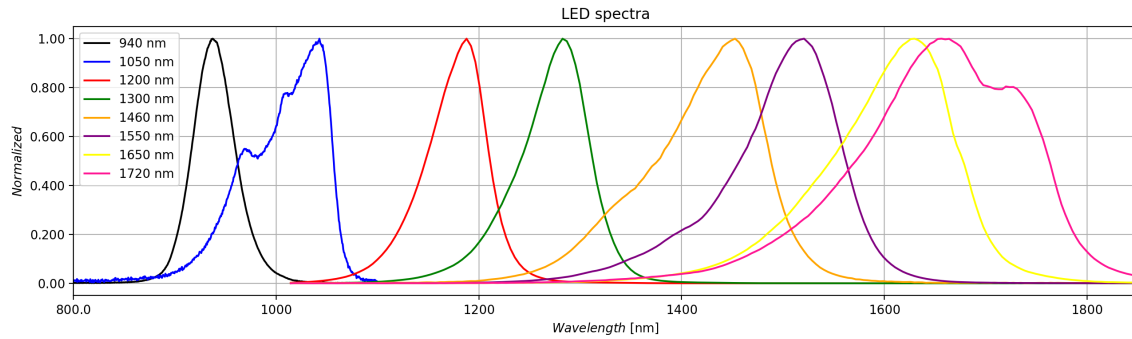
## 4 Results

Within this section the results of the characterisation of the LEDs and InGaAs detector are presented. The results of the reflection spectra of the different types of plastic and the differences in measuring with the plastic scanner versus the NIR spectrometer will be discussed.

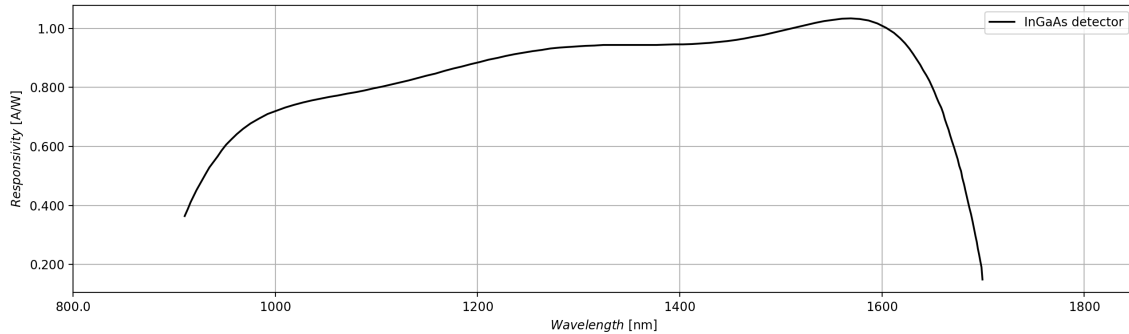
### 4.1 LEDs and InGaAs detector characterisation

To determine if the spectra, Full Width Half Maximum (FWHM) and the peak wavelength of the LEDs are chosen correctly to identify the types of plastic with the plastic scanner, the spectra of the LEDs have been measured using a spectrometer. The results of this experiment are presented in this paragraph.

The spectra of the 940 nm and the 1050 nm LEDs have been measured using a spectrometer with a detection range between 300 nm and 1100 nm. The spectra of the 1200 nm to 1720 nm LEDs have been measured with a NIR spectrometer with a detection range between 1000 nm and 2000 nm. The spectra of all LEDs are plotted in a single graph presented in figure 4.1a. The responsivity of the InGaAs is plotted in 4.1b.



(a) The measured LED spectra plotted in a single graph. The reflectance has been normalised.



(b) The responsivity of the InGaAs detector plotted with the extracted data from the data sheet.

Figure 4.1: The spectra of the LEDs and the responsivity of the InGaAs detector plotted with the same x-axis. (a) shows that the spectra overlap over a range of 900 nm to 1800 nm except at around 1100 nm and around 1350 nm. The spectra of the 1650 nm LED and the 1720 nm LED overlap almost entirely. (b) shows the responsivity of the InGaAs detector over a range of 900 nm to 1800 nm.

The x-axis of both figures are equal to represent how much of the spectra of the LEDs can be detected by the detector. Figure 4.1a shows the normalised spectra of the 8 different LEDs. The figure shows that the spectra overlap at most wavelengths except around 1350 nm and even less at 1100 nm. The spectra of the 1650 nm and 1720 nm LEDs overlap almost entirely. Considering the responsivity of the detector, figure 4.1 shows that the spectra of the 1650 nm and 1720 nm LEDs cannot be fully detected by the detector as well as the spectra of the 940 nm LED. The detection area of these LEDs are drawn in figure B.1, shown in Appendix B.

The responsivity of the data sheet starts at 900 nm compared to the 800 nm of the responsivity in the theory. The highest responsivity is around 1550 nm which corresponds with the highest responsivity of the theory.

To determine whether the measured spectra match the spectra obtained from the data sheet, the FWHM values and the peak values of the wavelengths are compared.

Figure 4.2 and table 4.1 show the comparison between the determined values and the values from the data sheet.

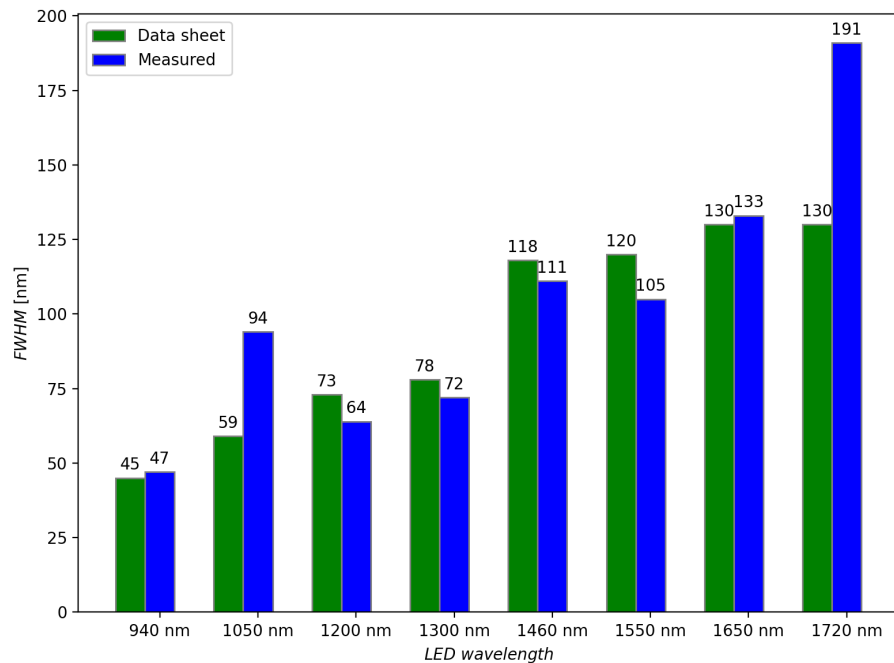


Figure 4.2: The FWHM values plotted as a bar graph to visualise the deviation between the determined values and the values obtained from the data sheet.

It was to be expected that the determined FWHM values would correspond with the FWHM values obtained from the data sheet. However, it can be seen in figure 4.2 that the deviations vary between 2 nm and 61 nm. The 1720 nm LED has the largest deviation from the data sheet.

The peak wavelengths of both the determined values as the obtained values from the data sheet are presented in table 4.1.

Table 4.1: The peak wavelengths values of the 8 different LEDs. The values of the measured peak wavelengths and the peak wavelengths collected from the data sheets are presented side by side. The deviation between the values are shown in the third column.

Peak wavelength from the data sheet (nm)	Measured peak wavelength (nm)	Deviation between the measured data and the datasheet (nm)
940	937	3
1050	1043	7
1200	1188	12
1300	1283	17
1460	1453	7
1550	1521	29
1650	1630	20
1720	1656	64

The deviations between the obtained and determined values vary between 3 nm and 64 nm. This is not as expected. The 1720 nm LED has the largest deviation of 64 nm. The 940 nm LED has the smallest deviation of 3 nm. For all LEDs the measured peak wavelengths is lower than the peak wavelengths obtained from the data sheet.

## 4.2 Plastic identification

To determine the spectra of the plastic samples, the samples have been measured with a halogen light and LEDs as a light source, where the NIR spectrometer was used as the detector. The samples have also been measured using a prototype of the plastic scanner, where the LEDs are used as a light source with the InGaAs detector as the detector. The reference tile of the Plastic Scanner was used as the reference tile for under or atop of the plastic samples. The spectra of the types of plastic of the three different experiments are shown in figure 4.3.

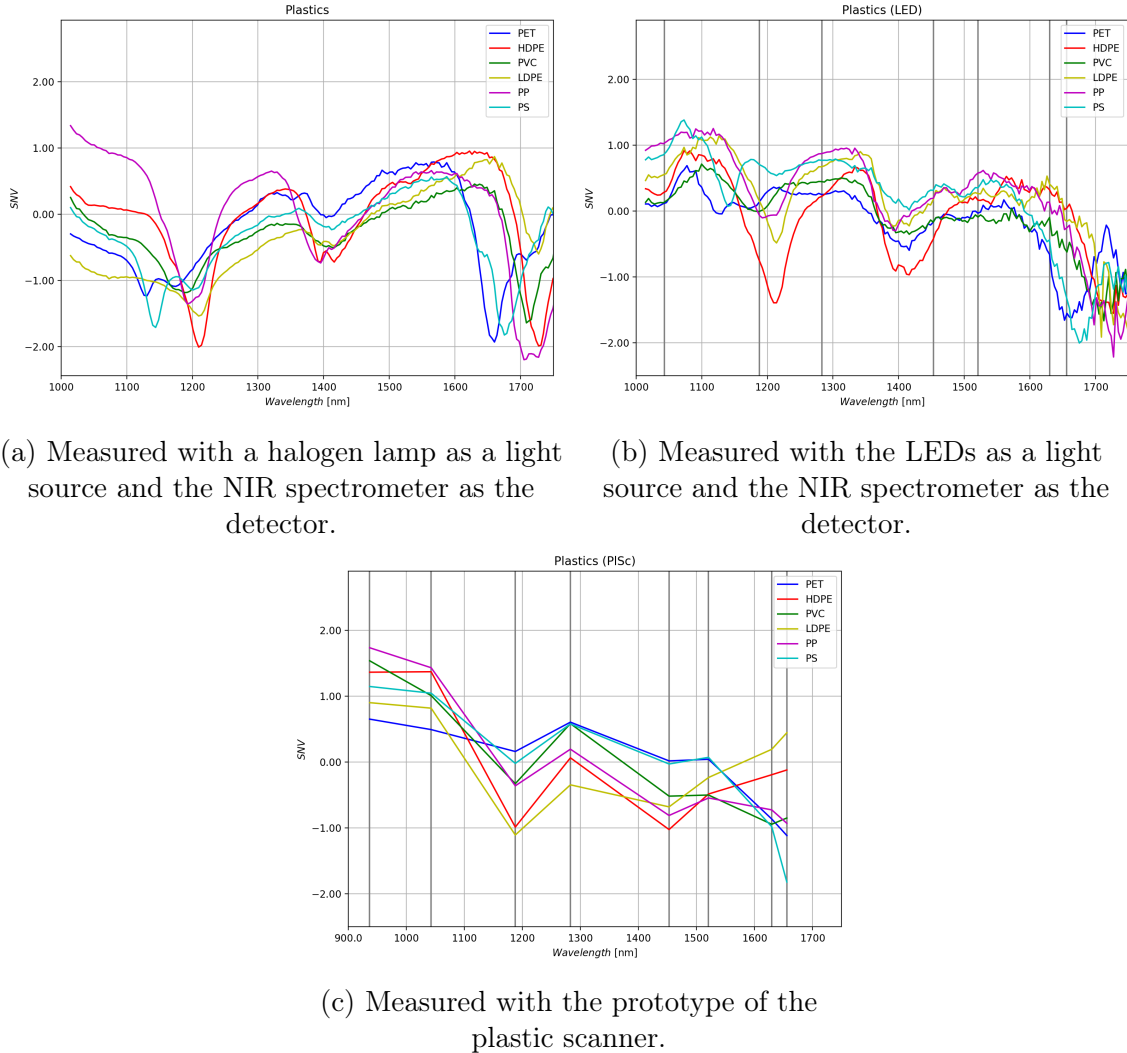


Figure 4.3: The spectra of the different types of plastic are plotted against the wavelength. (a) are the spectra of the types of plastic measured with a halogen lamp, (b) are the spectra measured with the NIR LEDs and (c) are the spectra measured using the plastic scanner prototype. A SNV-filter was applied to the plotted data sets. The grey lines plotted in (b) and (c) are the peak wavelength values of the LEDs. The enlarged figures of (a), (b) and (c) can be found in Appendix A.

Figure 4.3a shows that the identification dips of the types of plastic are between 1100 nm and 1250 nm, around 1400 nm and between 1600 nm and 1750 nm. Figure 4.3b also shows the identification dips around 1400 nm and between 1600 nm and 1750 nm. The dips between 1100 nm and 1250 nm that are visible in figure 4.3a are in figure 4.3b more centred around the 1200 nm. Figure 4.3b also shows that there is noise present in the reflected spectra around 1100 nm and the 1650 nm and 1720 nm LEDs. Figure 4.3c shows that the plastics can be best distinguished looking at the spectra at 937 nm and 1656 nm. At these wavelengths the spectra do not overlap with each other.

To determine if the measured spectra belong to the type of plastic, the spectra are compared to the theory. The theoretic spectra are shown in figure 2.4. Figure 2.4 shows that the 940 nm LED in the plastic scanner is needed to distinguish the spectrum of the HDPE from the spectrum of the PVC. However, the dip is not visible in the results measured with the spectrometer because of the detection limit of the NIR spectrometer.

#### 4.2.1 Plastic characteristics

From each type of plastic not every samples should be used for the reference box. The following samples in table 4.2 show a spectrum that do not show all of the identification dips to distinguish the types of plastic:

Table 4.2: The sample codes of the plastic samples that cannot be used as a reference for the plastic scanner. The colours of these samples are presented too.

Sample code	Colour
A05C	green
B05C	grey
C05C	blue
C06C	grey
D01C	white
D02C	transparent
F02C	blue

The spectra of these samples can be found in appendix C. For most samples the darker coloured samples have a less defined spectrum, except for the two samples of LDPE (D01C and D02C).

### 4.3 Discussion

As seen in figure 4.1a the spectra of the 1650 nm and 1720 nm LEDs overlap almost entirely. For this reason, it could be considered removing one of the LEDs from the design. However, both LEDs do not produce a high radiance to illuminate the plastic samples. This can be seen in the noise in figure 4.3b. Therefore, it would be suggested to remove the 1720 nm LED and increase radiance of the 1650 nm LED by replacing the LED with a LED with a higher power output.

The intensity of the reflected spectra are lowest around 1100 nm and around 1700 nm. Around 1700 nm, the power emitted by the 1650 nm and 1720 nm LEDs is 2 to 3 times lower than the LEDs with the wavelengths range from 940 nm to 1550 nm. Around 1100 nm the spectra of the 1050 nm and 1200 nm LEDs do not overlap, which results in a low intensity. Appendix D shows the intensity of the 8 different LEDs measured with the spectrometer and the power output obtained from the data sheets

with the corresponding viewing angle. The measured power output of the LEDs is an indication, due to the aligning of the LEDs into the optical fibre.

Figures 4.3a and 4.3b show for all spectra a dip around the 1400 nm. This suggests that it would be more beneficial to replace the 1460 nm LED with a 1400 nm LED to gain more intensity around the identification dip.

When measuring the spectra of the plastic samples, the samples were placed at a distance of 10 mm from the measurement surface. This distance was not always obtained with the experiments in which the spectra were measured with the NIR spectrometer. However, the distance could be obtained with the plastic scanner because of the integrated spacer. The intensity of the reflected spectra varied, but the shapes of the spectra corresponded, except for the samples presented in table 4.2.

The less defined spectra of the samples of table 4.2 are caused by the substance used to colour the plastic samples. Infrared light is absorbed by C-bonds. When a plastic sample is coloured with a substance in which C-bonds are present, more IR light can be absorbed by the plastic sample. A reason for the undefined spectra of the lighter coloured LDPE samples in table 4.2, could be of the thickness of the samples. The samples had a thickness smaller than 1 mm, which causes the NIR light to mostly pass through the sample and be reflected on the reference tile, after which the light is again partly absorbed by the sample before reaching the detector. Therefore, the spectra of the samples are a combination of the reflected spectra of the reference tile and the absorbance of the plastic samples.

## 5 Conclusion

This section discusses whether the correct wavelengths were chosen for the LEDs and if the spectra fit within the detection range of the detector. It also discussed the conclusions drawn from the results to determine which plastic samples are suitable for the reference box. The section ends with recommendation that could help with the future of the development of the plastic scanner.

The results show that the wavelengths for the LEDs were chosen correctly, except for the 1460 nm, 1650 nm and 1720 nm LEDs. As seen in the results a more defined identification dip is visible around 1400 nm. Replacing the 1460 nm LED with a 1400 nm LED will increase the intensity of the reflection around the identification dip to better distinguish the types of plastic. Furthermore, the results show that the spectra of the LEDs of 1650 nm and 1720 nm overlap. Despite the overlap, the intensity of both LEDs is lower than that of the other LEDs, creating noise in the spectra of the plastic types. To decrease the noise occurring in the spectra, it would be recommended to increase the intensity of the LEDs.

The results show that the range of the InGaAs detector is smaller than the range of the spectra of the LEDs. This means that not all reflected light is detected by the detector. This is especially noticeable around 1700 nm, where the noise in the spectra becomes more apparent. Because the spectra of the 1650 nm and 1720 nm LEDs overlap and are partly outside the detector range, removing one of the LEDs from the design could be considered to reduce costs. Moreover, the results show that between 1650 nm and 1750 nm an identification dip of the plastic types occurs. These dips are partly outside the range of the detector; therefore, replacing the detector with a detector with a wider range from 900 nm to 1750 nm should be considered.

It can be seen from the identification measurements that not all plastic samples can be used as references. Each type of plastic has at least one sample that cannot be used as a reference, except for the PP samples, where all samples can be used as references. Most samples are dark coloured, which explains the less defined spectra, however, the samples of LDPE are white and transparent. A reason for these samples to reflect a less defined spectrum could be of the thickness of the samples. It would be recommended to remove these samples from the reference box.

### 5.1 Recommendations

To improve the design of the plastic scanner a few recommendation can be given.

It is recommended to replace the 1460 nm LED with a 1400 nm LED to better distinguish the types of plastic around that identification dip around 1400 nm. It would also be wise to replace the 1650 nm LED with a higher power emitting 1650 nm LED.

It is recommended that the 1720 nm LED be removed from the design because the spectrum of the LED overlaps with the spectrum of the 1650 nm LED. The spectrum

of the 1650 nm LED covers the area over which the identification dip around 1700 nm can be measured. The 1650 nm LED is also lower in cost than the 1720 nm LED, resulting in lower manufacturing costs.

It would be recommended to remove the plastic samples, A05C, B05C, C05C, C06C, D01C, D02C and F02C, from the reference box, as the samples do not provide a suitable spectra to identify the types of plastic.

The plastic samples were measured with a reference tile under or on top of the sample to reflect the light passing through the sample. The reference tile provided by Plastic Scanner has been used for this purpose. In addition to this tile, four other tiles were measured to determine which tile reflected the most. This experiment was not pursued further due to lack of time. As a follow-up study, it would be useful to explore this further so that the right reference tile can be used to measure the plastic samples.

## References

- [1] L. Parker, "The world's plastic pollution crisis explained," *Environment*, May 2021. [Online]. Available: <https://www.nationalgeographic.com/environment/article/plastic-pollution>
- [2] "Plastic Scanner. | Plastic Scanner," Apr. 2023, [Online; accessed 26. Apr. 2023]. [Online]. Available: <https://plasticscanner.com>
- [3] "Plastic Waste and Pollution [Everything You Need To Know In 2020]," Nov. 2022, [Online; accessed 16. May 2023]. [Online]. Available: <https://cleanstreets.westminster.gov.uk/plastic-waste-complete-guide/#2>
- [4] admin, "Plastics – Resin Codes. What do they mean? - 2EA," *2EA*, Jan. 2018. [Online]. Available: <https://2ea.co.uk/plastics-resin-codes-what-do-they-mean>
- [5] "Plastic Recycling Codes & Symbols Explained - Plastic Soup Foundation," May 2020, [Online; accessed 16. May 2023]. [Online]. Available: <https://www.plasticsoupfoundation.org/en/plastic-problem/what-is-plastic/recycling-codes>
- [6] J. de Vos, "Plastic Identification Anywhere: Development of open-source tools to simplify plastic sorting," 2021, [Online; accessed 1. Jun. 2023]. [Online]. Available: <https://repository.tudelft.nl/islandora/object/uuid%3A1fa997b7-c286-4cf3-b3cc-4cfca7cf58f2?collection=education>
- [7] A. Straller and B. Gessler, "Identification of Plastic Types Using Discrete Near Infrared Reflectance Spectroscopy," *ResearchGate*, Dec. 2019. [Online]. Available: [https://www.researchgate.net/publication/337868860\\_Identification\\_of\\_Plastic\\_Types\\_Using\\_Discrete\\_Near\\_Infrared\\_Spectroscopy](https://www.researchgate.net/publication/337868860_Identification_of_Plastic_Types_Using_Discrete_Near_Infrared_Spectroscopy)
- [8] "About | Plastic Scanner," Jan. 2023, [Online; accessed 9. Feb. 2023]. [Online]. Available: <https://plasticscanner.com/about>
- [9] N. Gorretta, A. A. Gowen, N. Holden, M. Wolfe, J. Ogejo, and E. E. Cummins, "Visible and near infrared optical spectroscopy sensors for biosystems engineering," in *Introduction to Biosystems Engineering*. American Society of Agricultural and Biological Engineers (ASABE), 2020.
- [10] "Overview | Plastic Scanner documentation," May 2023, [Online; accessed 16. May 2023]. [Online]. Available: <https://docs.plasticscanner.com>
- [11] "Science of Plastics," Nov. 2019, [Online; accessed 9. Feb. 2023]. [Online]. Available: <https://www.sciencehistory.org/science-of-plastics>
- [12] "An Introduction to Plastics - Chemical Safety Facts," Oct. 2022, [Online; accessed 9. May 2023]. [Online]. Available: <https://www.chemicalsafetyfacts.org/chemistry-101/an-introduction-to-plastics>
- [13] NPO Kennis, "Wat is plastic en hoe maak je het?" *NPO Kennis*, Jan. 2022. [Online]. Available: <https://npokennis.nl/longread/7956/wat-is-plastic-en-hoe-maak-je-het>

- [14] “Polyethylene Terephthalate - an overview | ScienceDirect Topics,” Feb. 2023, [Online; accessed 9. Feb. 2023].
- [15] “Polyvinyl Chloride Structure & Uses | What is PVC? | Study.com,” Feb. 2023, [Online; accessed 9. Feb. 2023]. [Online]. Available: <https://study.com/learn/lesson/what-is-polyvinyl-chloride-pvc-structure-uses.html>
- [16] “Polypropylene (PP) - Types, Properties, Uses & Structure,” Feb. 2023, [Online; accessed 9. Feb. 2023]. [Online]. Available: <https://omnexus.specialchem.com/selection-guide/polypropylene-pp-plastic>
- [17] “A Polystyrene Model of Polystyrene Tacticity,” Nov. 2021, [Online; accessed 9. Feb. 2023]. [Online]. Available: <https://www.chemedx.org/blog/polystyrene-model-polystyrene-tacticity>
- [18] “Polyethylene (PE) - Properties, Uses & Application,” Feb. 2023, [Online; accessed 9. Feb. 2023]. [Online]. Available: <https://omnexus.specialchem.com/selection-guide/polyethylene-plastic>
- [19] D. ir. M.T.C. de Loos-Vollebregt, *Spectrometrische analysetechnieken*. Arnhem: Syntax Media, 2009.
- [20] O. c. Tutor, “Infrared Spectroscopy - Online Organic Chemistry Tutor,” *Online Organic Chemistry Tutor*, Nov. 2017. [Online]. Available: <https://onlineorganicchemistrytutor.com/infrared-spectroscopy>
- [21] H. Masoumi, S. M. Safavi, and Z. Khani, “Identification and classification of plastic resins using near infrared reflectance spectroscopy,” *International Journal of Mechanical and Industrial Engineering*, vol. 6, pp. 213–220, 2012.
- [22] “Infrared Spectroscopy,” Dec. 2010, [Online; accessed 23. May 2023]. [Online]. Available: <https://www.ru.nl/systemschemistry/equipment/optical-spectroscopy/infrared>
- [23] “What is Spectroscopy? - Avantes,” Sep. 2022, [Online; accessed 23. May 2023]. [Online]. Available: <https://www.avantes.com/what-is-spectroscopy>
- [24] S. Kasap, *Optoelectronics and Photonics: Principles and Practices*, 2nd ed. Pearson Education Limited, 2013, ch. 3.
- [25] D. C. Giancoli, *Physics for Scientists & Engineers with Modern Physics*, 4th ed. Pearson Education Inc., 2009, ch. 40.
- [26] S. Kasap, *Optoelectronics and Photonics: Principles and Practices*, 2nd ed. Pearson Education Limited, 2013, ch. 5.
- [27] A. Rohatgi, “WebPlotDigitizer - Copyright 2010-2022 Ankit Rohatgi,” Sep. 2022, [Online; accessed 21. Apr. 2023]. [Online]. Available: <https://apps.automeris.io/wpd>

- [28] Bijdragers aan Wikimedia projecten, “Standard Normal Variate - Wikipedia,” Apr. 2017, [Online; accessed 15. May 2023]. [Online]. Available: [https://nl.wikipedia.org/w/index.php?title=Standard\\_Normal\\_Variate&oldid=48942585](https://nl.wikipedia.org/w/index.php?title=Standard_Normal_Variate&oldid=48942585)
- [29] “Plastic-Scanner · GitHub,” May 2023, [Online; accessed 11. May 2023]. [Online]. Available: <https://github.com/Plastic-Scanner>

# Appendices

## A Enlarged figures

Enlarged figures of the screenshot of the PSplot software and the figures from section 4.2.

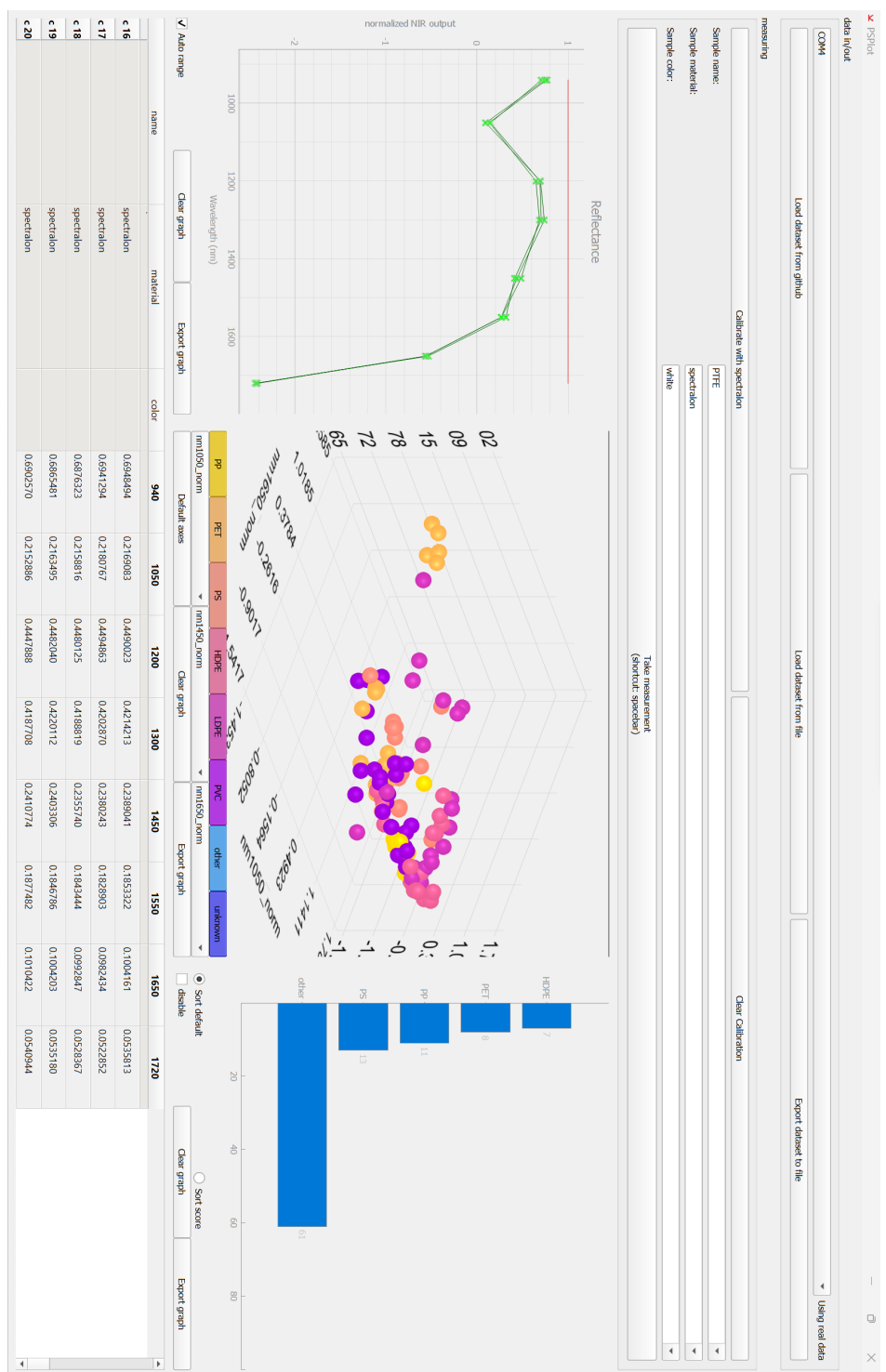


Figure A.1: An enlarged figure of the PS plot software presented in figure 3.9. The PS plot software to identify the different types of plastic.

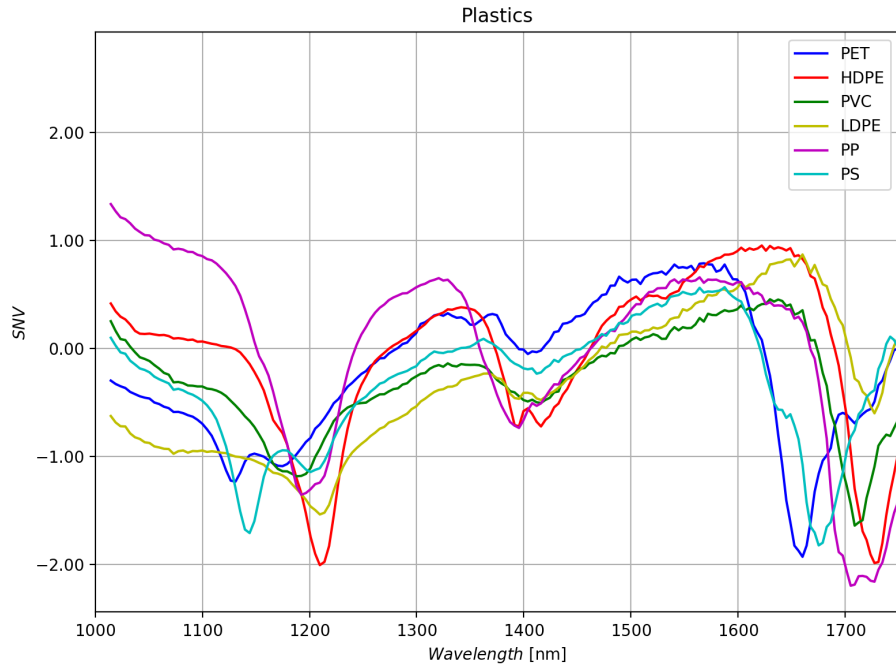


Figure A.2: An enlarged figure of figure 4.3a.

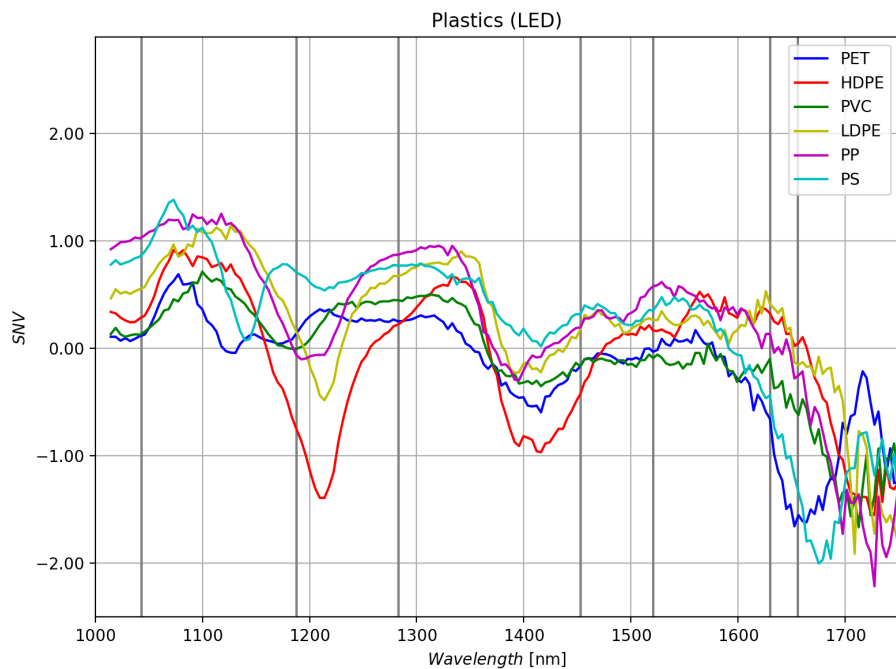


Figure A.3: An enlarged figure of figure 4.3b.

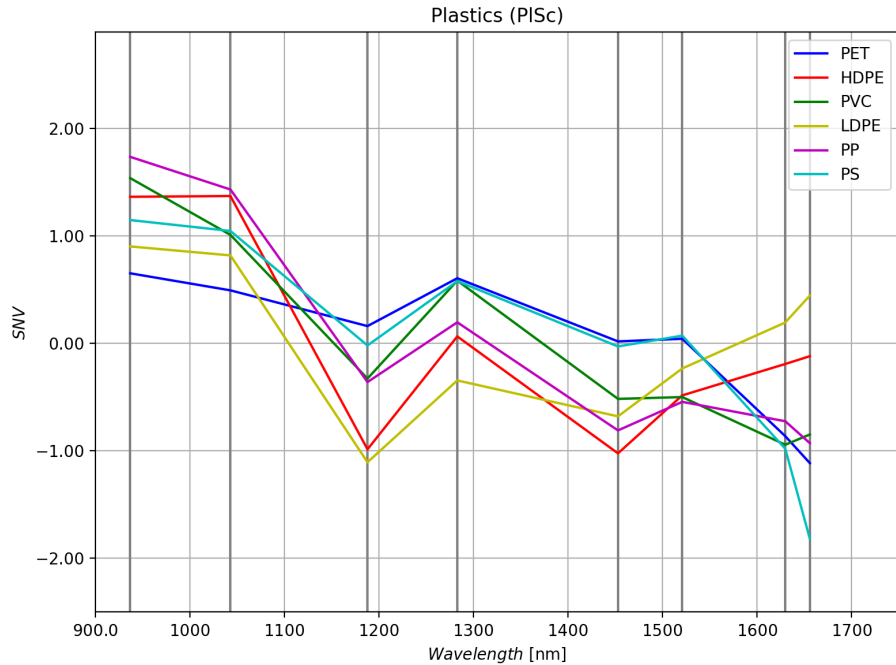


Figure A.4: An enlarged figure of figure 4.3c.

## B Spectra detection

The responsivity of the InGaAs detector has been plotted in the same graph as the spectra of the NIR LEDs, see figure B.1.

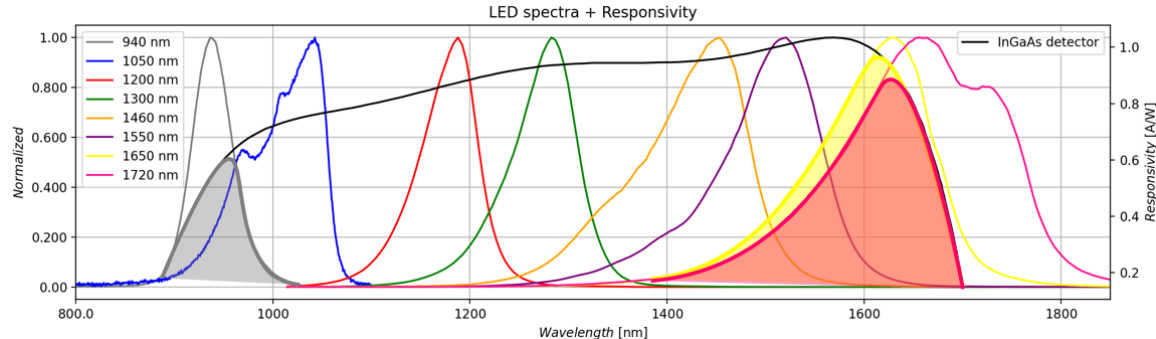


Figure B.1: The spectra of the 8 different LEDs and responsivity of the InGaAs detector are plotted against the wavelength. The left y-axis The coloured areas show how much the spectra of the LEDs are detected by the detector.

Figure B.1 shows that the spectra of the 940 nm, 1650 nm and 1720 nm LEDs are outside the responsivity of the InGaAs detector. The area of the spectra that is still detected by the detector is shown in grey for the 940 nm LED, yellow for the 1650 nm LED and deeppink for the 1720 nm LED. This suggest that either the 1650 nm or the 1720 nm LED can be removed from the design. Due to the larger range of the spectra of the 1650 nm LED that can be detected by the detector, it is recommended to remove the 1720 nm LED.

It would be beneficial to keep the 940 nm LED in the design as HDPE shows an identification dip around 950 nm.

## C Figures of the plastic characteristics

The spectra of the samples of the types of plastic are plotted in individual graphs in which the legend shows which colour belongs to which sample. The letters after the underscore of the sample code indicate the colour of the sample. Table C.1 shows which letters belong to which colour.

Table C.1: The colours of the plastic samples belonging to the letters presented in the legend of the figures in Appendix C.

Letters	Colour
w	white
t	transparent
g	green
wt	white transparent
y	yellow
gr	grey
bl	blue
r	red
p	purple

The following figures show the spectra of the samples of the different types of plastic. The legend shows the colour next to the sample codes of the plastic samples.

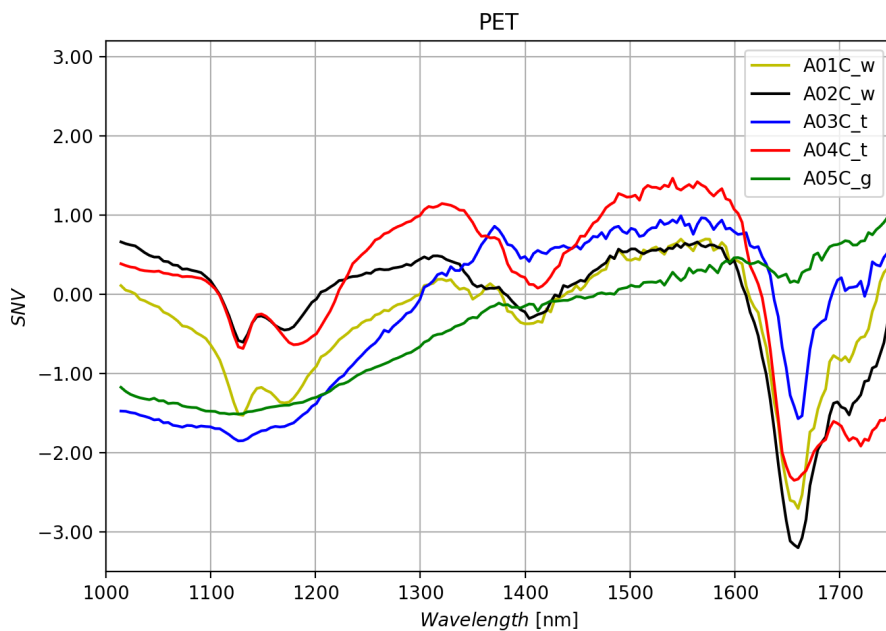


Figure C.1: The spectra of the five samples of PET. The legend shows the sample code with after the underscore the colour of the sample.

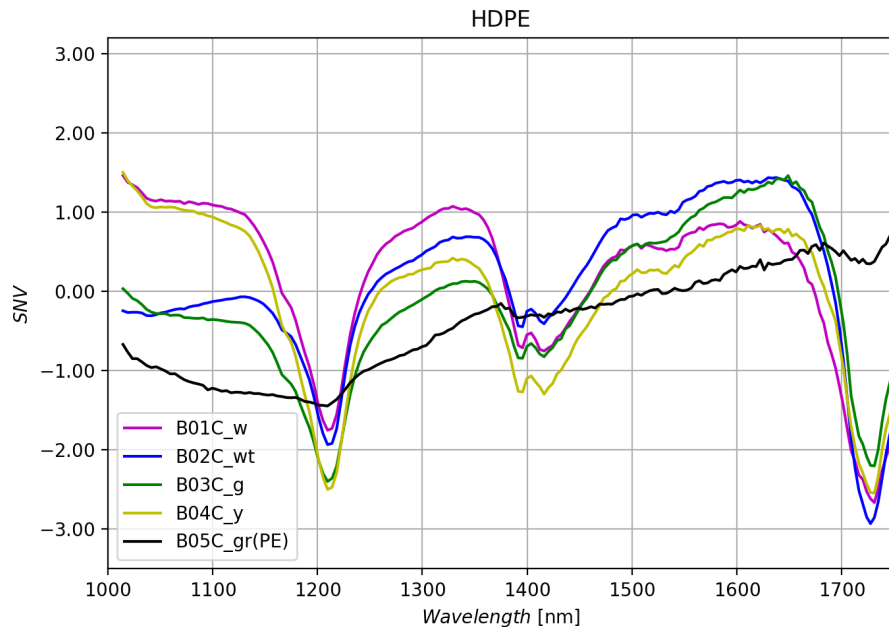


Figure C.2: The spectra of the five samples of HDPE. The legend shows the sample code with after the underscore the colour of the sample

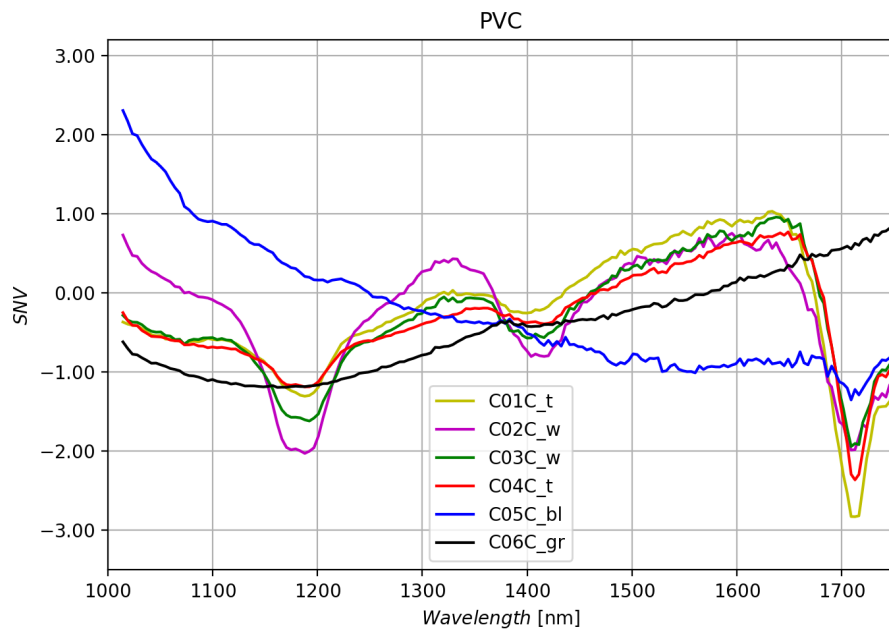


Figure C.3: The spectra of the six samples of PVC. The legend shows the sample code with after the underscore the colour of the sample

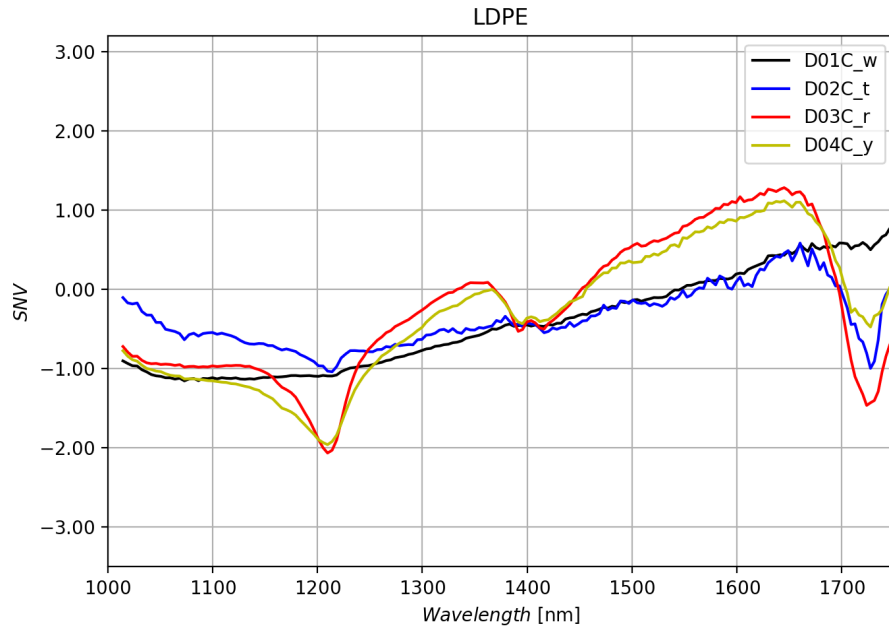


Figure C.4: The spectra of the four samples of LDPE. The legend shows the sample code with after the underscore the colour of the sample

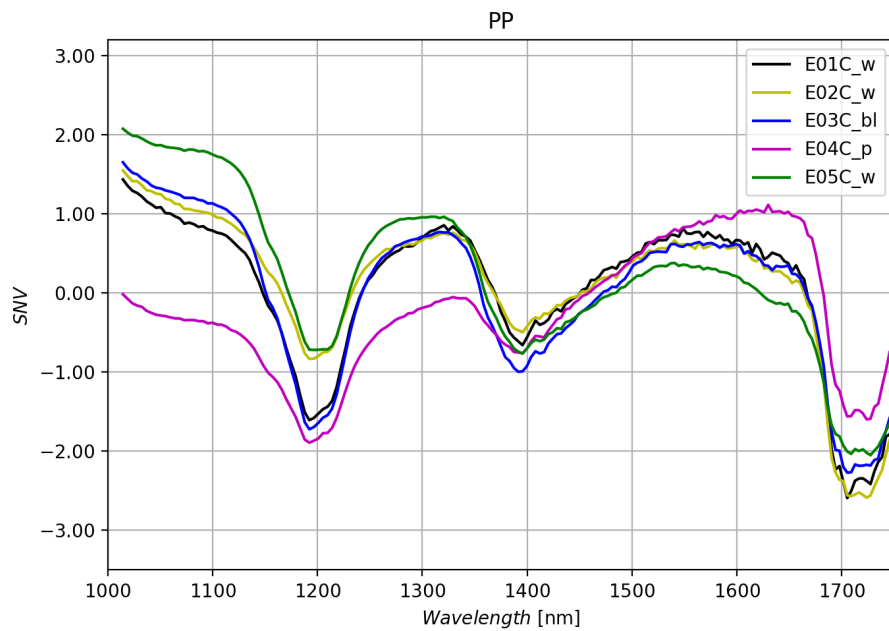


Figure C.5: The spectra of the five samples of PP. The legend shows the sample code with after the underscore the colour of the sample

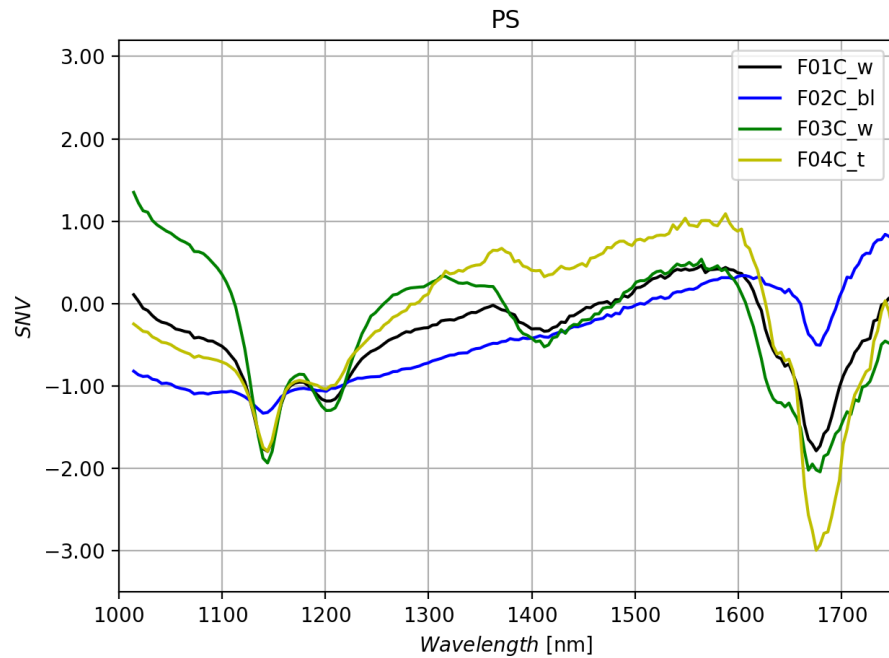


Figure C.6: The spectra of the four samples of PS. The legend shows the sample code with after the underscore the colour of the sample

## D Intensity LEDs spectra

The light of the LEDs is emitted in an angle with a certain power output. The power output was obtained during the measurement to determine the spectra of the LEDs. The intensity is presented in counts in figure D.1.

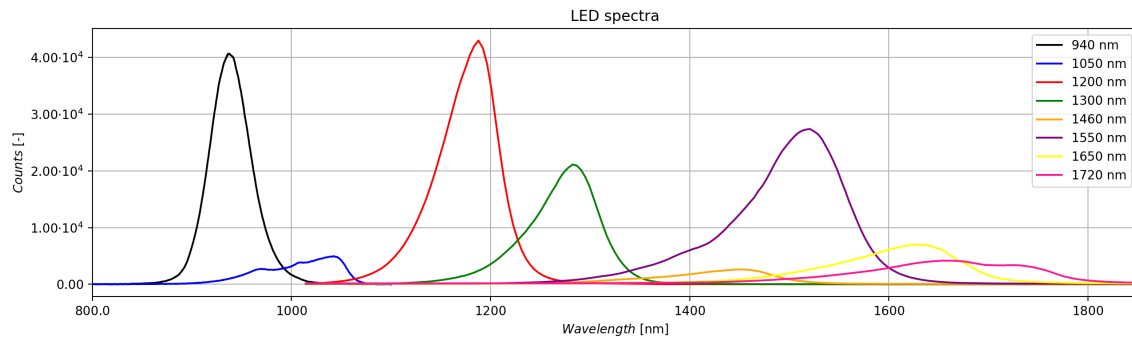


Figure D.1: The measured intensity of the spectra from the NIR LEDs in counts.

Figure D.1 shows that the intensity of the 940 nm, 1200 nm, 1300 nm and the 1550 nm LEDs are the highest. The intensity of the other LEDs are almost undetectable compared to the intensity of the earlier mentioned LEDs. The measured intensity is relative because of the aligning of the LEDs into the fibre.

Table D.1: The obtained power output of the LEDs from the data sheets with the corresponding viewing angle.

LED	Power output (mW)	Power angle (deg)
1050 nm	11	50
1200 nm	12	40
1300 nm	11	40
1460 nm	6	40
1550 nm	6	40
1650 nm	3	50
1720 nm	3	120